

LUMINESCENCE SPECTRA OF TOLUENE,  
BENZYL RADICAL AND SOME OF THEIR  
DEUTERATED ANALOGUES

LUMINESCENCE SPECTRA OF TOLUENE,  
BENZYL RADICAL AND SOME OF THEIR  
DEUTERATED ANALOGUES

By

VINCENT JOSEPH MORRISON, B.Sc.

A Thesis

Submitted to the School of Graduate Studies  
in Partial Fulfillment of the Requirements  
for the Degree  
Master of Science

McMaster University

May 1975

MASTER OF SCIENCE  
(Chemistry)

McMASTER UNIVERSITY  
Hamilton, Ontario

TITLE: Luminescence Spectra of Toluene, Benzyl Radical and Some of  
Their Deuterated Analogues

AUTHOR: Vincent Joseph Morrison, B.Sc. (Saint Francis Xavier University)

SUPERVISOR: Dr. Joseph D. Laposa

NUMBER OF PAGES: ix , 87

## ACKNOWLEDGEMENTS

I would like to express my special thanks to my parents and to my aunt, Mary MacLean MacDonald. Without their support and encouragement this work would not have been possible.

I wish to thank my research supervisor, Dr. J.D. Laposa, for suggesting this work and for his encouragement and assistance in the preparation of this thesis.

I am also grateful to fellow graduate students Hal Singh and Dave Condirston for encouragement and helpful discussions.

Finally, I am indebted to Veronica Komczynski and Jan Gallo for their excellent typing, to the Chemistry Department of McMaster University for financial support and also to my friends at McMaster for making my stay here a pleasant one.

## TABLE OF CONTENTS

|  | Page |
|--|------|
| CHAPTER I  | 1    |
| INTRODUCTION   |      |
| CHAPTER II   | 4    |
| THEORY   |      |
| 2.1  | 4    |
| Symmetry Classification of Toluene and<br>Benzyl Radical |      |
| 2.2  | 6    |
| Spectroscopic Transitions                                |      |
| 2.3  | 8    |
| Vibrations of Polyatomic Molecules                       |      |
| 2.4  | 8    |
| Isotope Effect   |      |
| 2.5  | 9    |
| The Born-Oppenheimer Approximation                       |      |
| 2.6  | 11   |
| Classification of Electronic States                      |      |
| 2.7  | 13   |
| Theory of Electronic Transitions                         |      |
| 2.8  | 15   |
| Vibronic Coupling  |      |
| 2.9  | 17   |
| The Franck-Condon Principle                              |      |
| 2.10   | 19   |
| Fluorescence and Phosphorescence                         |      |
| 2.11   | 23   |
| Characteristics of Polycrystalline Matrices              |      |
| CHAPTER III  | 28   |
| EXPERIMENTAL   |      |
| 3.1  | 28   |
| Chemicals  |      |
| 3.2  | 29   |
| Solvents   |      |
| 3.3  | 29   |
| Apparatus  |      |
| CHAPTER IV   | 32   |
| RESULTS AND DISCUSSION                                   |      |
| 4.1  | 37   |
| Vibrational Analysis of Phosphorescence<br>of Toluenes   |      |
| 4.2  | 48   |
| Discussion of Phosphorescence of Toluene                 |      |
| 4.3  | 53   |
| Vibrational Analysis of Fluorescence                     |      |

|  | Page |
|--|------|
| 4.4 Discussion of Fluorescence of Toluene                      | 67   |
| 4.5 Vibrational Analysis of Fluorescence<br>of Benzyl Radicals | 71   |
| 4.6 Discussion of Fluorescence of Benzyl<br>Radical            | 81   |
| CHAPTER V SUMMARY  | 86   |
| REFERENCES   | 88   |

## LIST OF TABLES

|           |  | Page |
|-----------|--|------|
| Table 2.1 | Character Table for Point Group $C_{2v}$   | 7    |
| Table 2.2 | Direct Product Table for Point Group $C_{2v}$  | 7    |
| Table 2.3 | Rate Constants for Radiative and Non-Radiative Processes in Rigid Media at 77°K  | 24   |
| Table 4.1 | Ground State Fundamentals in Toluene and Some of its Deuterated Derivatives  | 34   |
| Table 4.2 | Description of Benzene Ring and Ring Substituent Vibrations of Toluene   | 36   |
| Table 4.3 | Vibrational Analyses of Phosphorescences of Toluene and Toluene- $\alpha$ -d3 in Polycrystalline Methylcyclohexane at 77°K         | 39   |
| Table 4.4 | Vibrational Analyses of Phosphorescences of Toluene-d8 and Toluene-d5 in Polycrystalline Methylcyclohexane at 77°K                 | 41   |
| Table 4.5 | Vibrational Analyses of Phosphorescences of Para, Meta, and Ortho-deuterated Toluenes in Polycrystalline Methylcyclohexane at 77°K | 46   |
| Table 4.6 | Vibrational Analyses of Fluorescences in Toluene and Toluene- $\alpha$ -d3 in Polycrystalline Methylcyclohexane at 77°K            | 56   |
| Table 4.7 | Vibrational Analyses of Fluorescences of Toluene-d5 and Toluene-d8 in Polycrystalline Methylcyclohexane at 77°K                    | 59   |
| Table 4.8 | Vibrational Analyses of Fluorescences of Para, Meta, and Ortho-deuterated Toluenes in Polycrystalline Methylcyclohexane at 77°K    | 64   |

|            |   | Page |
|------------|---|------|
| Table 4.9  | Vibrational Analyses of Fluorescences of Benzyl Radical and Benzyl Radical- $\alpha$ -d <sub>2</sub> in Polycrystalline Methylcyclohexane at 77°K     | 74   |
| Table 4.10 | Vibrational Analyses of Fluorescences of Benzyl Radical-d <sub>5</sub> and Benzyl Radical-d <sub>7</sub> in Polycrystalline Methylcyclohexane at 77°K | 76   |
| Table 4.11 | Vibrational Analyses of Fluorescences of Para, Meta, and Ortho-deuterated Benzyl Radicals in Polycrystalline Methylcyclohexane at 77°K                | 79   |

## LIST OF ILLUSTRATIONS

|               |   | Page |
|---------------|---|------|
| Figure 2.1    | Symmetry Elements of Toluene and Benzyl Radical   | 5    |
| Figure 2.2a,c | Franck-Condon Potential Energy Curves for the Ground and First Excited States   | 18   |
| Figure 2.2b,d | Expected Emission Progressions of Systems Depicted in Figure 2.3a,c   | 18   |
| Figure 2.3    | Jablonski Diagram Illustrating Different Mechanisms for the Intramolecular Loss of Energy   | 20   |
| Figure 2.4a   | Comparison of Gas Phase and Matrix Emissions  | 26   |
| Figure 2.4b   | Difference of 0,0 Energies for Absorption and Emission  | 26   |
| Figure 3.1    | Block Diagram of the Apparatus Used for Emission Experiments  | 30   |
| Figure 4.1    | Schematic Illustrations of Some Vibrational Modes of Monosubstituted Benzenes   | 33   |
| Figure 4.2    | Phosphorescence Spectra of Toluene, Toluene- $\alpha$ -d <sub>3</sub> , Toluene-d <sub>5</sub> and Toluene-d <sub>8</sub> in Methylcyclohexane Matrices at 77°K | 38   |
| Figure 4.3    | Phosphorescence Spectra of Toluene, Para-, Meta-, and Ortho-deuterated Toluenes in Methylcyclohexane Matrices at 77°K   | 45   |
| Figure 4.4    | Fluorescence Spectra of Toluene, Toluene- $\alpha$ -d <sub>3</sub> , Toluene-d <sub>5</sub> and Toluene-d <sub>8</sub> in Methylcyclohexane Matrices at 77°K    | 55   |

|            |  | Page |
|------------|--|------|
| Figure 4.5 | Fluorescence Spectra of Toluene, Para-, Meta-, and Ortho-deuterated Toluenes in Methylcyclohexane Matrices at 77°K   | 63   |
| Figure 4.6 | Fluorescence Spectra of Benzyl Radical, Benzyl Radical- $\alpha$ -d <sub>2</sub> , Benzyl Radical-d <sub>5</sub> , and Benzyl Radical-d <sub>7</sub> in Methylcyclohexane Matrices at 77°K | 73   |
| Figure 4.7 | Fluorescence Spectra of Benzyl Radical, Para-, Meta-, and Ortho-deuterated Benzyl Radicals in Methylcyclohexane Matrices at 77°K   | 78   |

TO MY PARENTS

## CHAPTER 1

### INTRODUCTION

A number of methods are available for obtaining information about the ground state geometries of molecules. However, the accumulation of geometry data for molecules in excited electronic states has been hindered by a shortage of reliable methods for obtaining such information. If the rotational fine structure of a vibronic absorption band is resolved, it can be studied to obtain rotational constants and thus the geometry of a molecule in an electronically excited state can be deduced. In many instances, however, such fine structure cannot be resolved so observations of sub-bands or the overall shape of the rotational bands is used. The molecules being studied must be present in the gas phase, of course.

Excited state geometries can be inferred on the basis of the Franck-Condon principle. According to this principle, for a transition between electronic states, the most prominent vibrational progressions are those arising from normal modes which convert the geometry of one state into that of the other. The Franck-Condon principle has been applied quantitatively by measuring the relative intensities of the bands of a progression for both absorption<sup>1,2</sup> and emission<sup>3</sup> spectra.

In this study the vibrational fine structure of the fluorescence spectra of toluene and benzyl radical, along with the phosphorescence

spectrum of toluene were analyzed. The solutes were imbedded in polycrystalline matrices at 77°K.

The spectroscopically observable effects of chemical substitution of benzene have been of interest for some time. The particular case of methyl substitution of benzene has been the subject of U.V. absorption,<sup>4,5,6</sup> singlet-triplet absorption,<sup>7</sup> low temperature phosphorescence experiments<sup>8,9,10</sup> and fluorescence studies in both the vapour phase<sup>11,12</sup> and polycrystalline matrices.<sup>13</sup> These workers<sup>10,13</sup> have included deuterium substituted toluenes in their studies, using the deuterium shifts of vibrational frequencies as an aid in assigning the vibrational structure of their emission spectra. It is known that features of the vibrational structure vary from solvent to solvent. Along with the determination of the most important progressions in the fluorescence and phosphorescence of toluene, this work involves the study of the prominence of forbidden components in allowed transitions.

Benzyl radical is one of the simplest and, at the same time, one of the most experimentally accessible aromatic free radicals. Schüler and co-workers<sup>14,15,16</sup> were the first to prepare benzyl radical and obtain its emission spectrum using gaseous toluene with an electric discharge being passed through it. A number of other workers<sup>17,18,19</sup> also obtained spectra of benzyl radical in this manner. Use of the discharge method leads to production of side products, however, so Norman and Porter<sup>20</sup> used the method of preparing free radicals in situ by photolysis of the parent substance dissolved in a hydrocarbon glass at low temperatures. Porter and co-workers<sup>20,21</sup> observed the absorption spectrum of benzyl radical after photolyzing toluene in hydrocarbon solvents at 77°K. The low

temperature fluorescence spectrum of benzyl in a polycrystalline matrix has been the subject of investigation,<sup>13,22</sup> and the excitation spectrum of benzyl radical has been observed<sup>23</sup> using a hydrocarbon matrix at 77°K. Photoselection data<sup>24</sup> obtained using a hydrocarbon matrix at 77°K and rotational contour analyses of several bands of the gas phase emission spectrum<sup>19</sup> were required in order to confirm the symmetry of the first excited doublet state as  $A_2$ . Deuterated analogues of benzyl radical have been used<sup>13,22</sup> in assigning the vibrational structure of its fluorescence at low temperature in a polycrystalline matrix and it is known that these spectra also are solvent dependent. In this study, the prominence of forbidden components in the allowed electronic transition is also considered.

## CHAPTER II

### THEORETICAL

#### 2.1 SYMMETRY CLASSIFICATION OF TOLUENE AND BENZYL RADICAL

Group theory has been a valuable asset in the understanding of spectral data. Examination of the symmetry elements of a molecule in its equilibrium nuclear configuration enables the assignment of the molecule to a symmetry point group.

Electron diffraction studies<sup>25</sup> indicate that the phenyl ring of toluene is essentially a planar hexagon. Microwave measurements show that the methyl group rotates quite freely, even in the condensed phase.<sup>26</sup> The incident electromagnetic radiation would therefore interact with the molecule with equal probability for all configurations of the methyl group with respect to the ring. Hence, the methyl group can be considered as an atom and the  $\text{CH}_2\cdot$  group of benzyl is assumed to behave as a single atom also.

In addition to the identity element, toluene possesses three additional symmetry elements: a two-fold rotation axis and two reflection planes. These three symmetry elements are shown in Fig. 2.1 where the axes have been defined according to Mulliken's convention.<sup>27</sup> The corresponding symmetry operations are:

$C_2(Z)$ : rotation through  $180^\circ$  about the Z axis;

$\sigma_v(XZ)$ : reflection in a plane perpendicular to the molecular plane;

$\sigma'_v(YZ)$ : reflection in a plane coincident with the molecular plane.

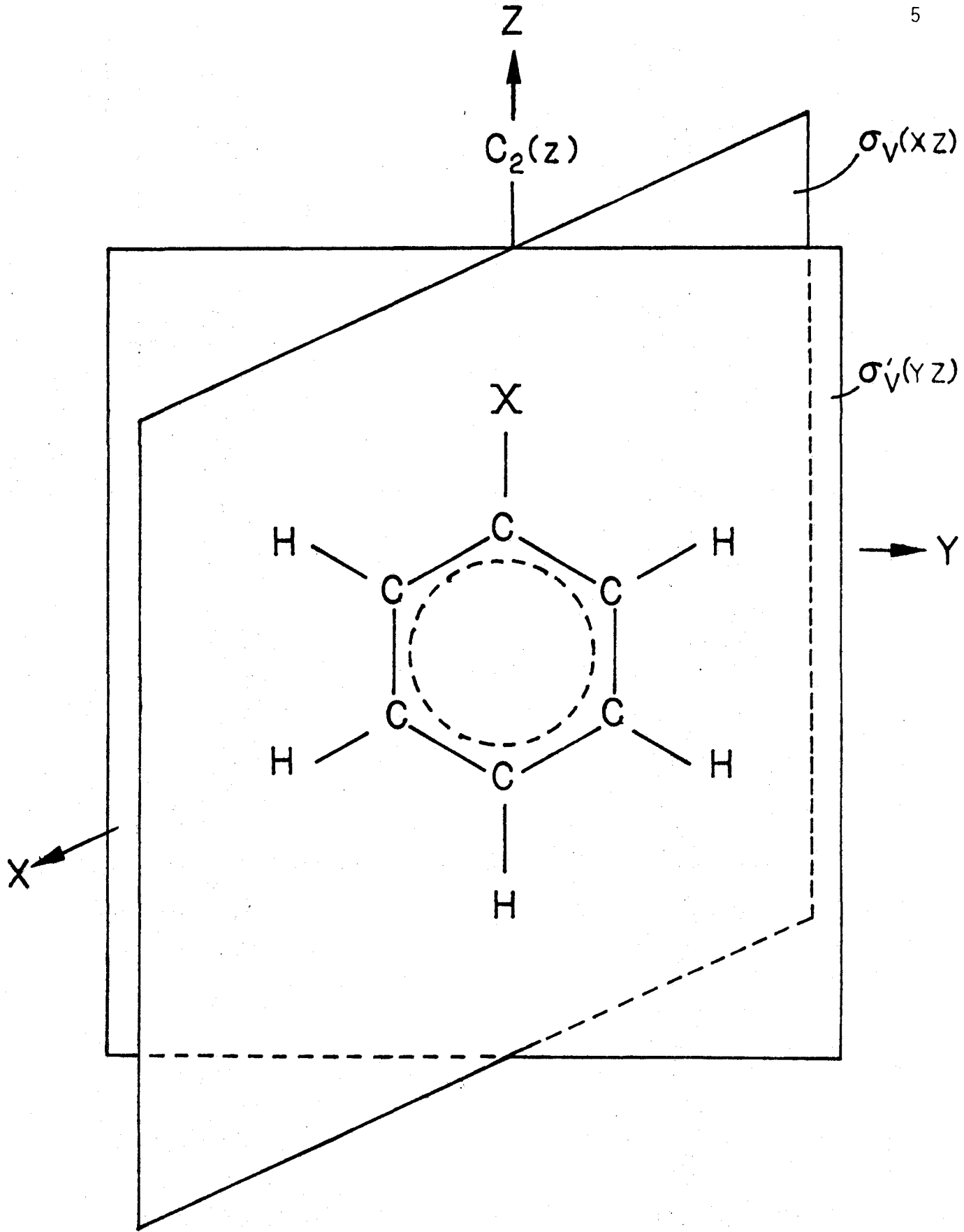


Figure 2.1 Symmetry elements of monosubstituted benzenes.

These symmetry operations are those of the point group  $C_{2v}$  and it is to that point group that toluene, toluene- $\alpha$ -d3, ring deuterated toluene-d5, toluene-d8 and the analogous benzyl radicals all belong. The same point group applies if there is monodeuteration in the para position but if the ortho or meta positions are deuterated, the resulting molecules can be considered as belonging to the point group  $C_s$ .

The character table and direct product table for  $C_{2v}$  are given in Tables 2.1 and 2.2. Such tables are helpful in determining which electronic transitions are symmetry allowed, and which vibrational modes are infrared and Raman active.

## 2.2 SPECTROSCOPIC TRANSITIONS

A spectroscopic transition can occur between two states  $E_i$  and  $E_f$  if

$$\Delta E = |E_f - E_i| = h\nu \quad (2.1)$$

where  $E_f$  and  $E_i$  are the energies of the final and initial states with respect to an arbitrary zero,  $\nu$  is the frequency of the absorbed or emitted photon and  $h$  is Planck's Constant. Equation(2.1) can be written in the form

$$\bar{\nu} = \frac{|E_f - E_i|}{hc} \quad (2.2)$$

where  $h$  (Planck's constant) =  $6.62 \times 10^{-27}$  erg-sec and  $C$  is the speed of light in a vacuum =  $3.00 \times 10^{10}$  cm sec<sup>-1</sup>.  $\bar{\nu}$  is the wave number of the electromagnetic radiation absorbed or emitted when the transition occurs and is expressed in reciprocal centimeters. It is equivalent to the reciprocal of the wavelength,  $\lambda$ , and is proportional to the energy of the photon.

TABLE 2.1

Character Table for Point Group  $C_{2v}$ 

| $C_{2v}$ | E | $C_2(z)$ | $\sigma_v(xz)$ | $\sigma_v(yz)$ |   |       |
|----------|---|----------|----------------|----------------|---|-------|
| $A_1$    | 1 | 1        | 1              | 1              | z |       |
| $A_2$    | 1 | 1        | -1             | -1             |   | $R_z$ |
| $B_1$    | 1 | -1       | 1              | -1             | x | $R_y$ |
| $B_2$    | 1 | -1       | -1             | 1              | y | $R_x$ |

TABLE 2.2

Direct Product Table for Point Group  $C_{2v}$ 

| $C_{2v}$ | $A_1$ | $A_2$ | $B_1$ | $B_2$ |
|----------|-------|-------|-------|-------|
| $A_1$    | $A_1$ | $A_2$ | $B_1$ | $B_2$ |
| $A_2$    | $A_2$ | $A_1$ | $B_2$ | $B_1$ |
| $B_1$    | $B_1$ | $B_2$ | $A_1$ | $A_2$ |
| $B_2$    | $B_2$ | $B_1$ | $A_2$ | $A_1$ |

### 2.3 VIBRATIONS OF POLYATOMIC MOLECULES

For molecules having  $N$  nuclei, there are  $3N$  degrees of freedom of motion. There are three rotational and three translational degrees of freedom for each molecule so there are  $3N-6$  vibrational degrees of freedom per molecule. (There are  $3N-5$  in a linear molecule which has only two rotational degrees of freedom.) Hence, in non-linear molecules, the vibrational motion can be resolved into  $3N-6$  normal modes, a normal mode being defined as a mode of vibration where each atom in the molecule reaches its position of maximum displacement at the same time and each atom passes through its equilibrium position at the same time.<sup>28</sup>

Including the methyl-ring torsional mode, there are thirty-nine normal modes in toluene (thirty-six in benzyl radical) and they are classified according to frequency and symmetry, the frequencies being called normal, or fundamental frequencies. There is a normal coordinate assigned to each normal mode and the vibrational motion of the molecule can be discussed in terms of these coordinates. The normal modes and frequencies for toluene are listed in Table 4.1. References (28), (29) and (30) treat the topic in detail.

### 2.4 ISOTOPE EFFECT

When an atom of a molecule is replaced by an isotopic atom of the same element, it is assumed that the potential energy function and configuration of the molecule are essentially the same.<sup>28,31</sup> The frequency of the vibration may be changed somewhat because of the change in mass. This is particularly true if hydrogen and deuterium are the atoms in question because there is a large percentage change in mass.

This frequency shift, or isotope effect, is useful in assigning spectral lines to modes of vibration. A given normal mode in which a hydrogen atom is oscillating with a relatively large amplitude, will undergo a greater change in frequency than a normal mode in which the hydrogen is vibrating with a smaller amplitude.

## 2.5 THE BORN-OPPENHEIMER APPROXIMATION

The operator form of the time-independent Schrödinger equation is

$$\hat{H}\psi_t = E_t\psi_t \quad (2.3)$$

where  $\psi_t$  is an eigenfunction corresponding to a stationary state of the system and is dependent upon the coordinates of all electrons and nuclei. The  $E_t$  values are the eigenvalues and correspond to the sum of potential and kinetic energies of the electrons and nuclei present.  $\hat{H}$  is referred to as the Hamiltonian operator and has the form

$$\hat{H} = \text{kinetic energy} + \text{potential energy} = \hat{T}_E + \hat{T}_N + \hat{V}_{EN} + \hat{V}_{NN} + \hat{V}_{EE} \quad (2.4)$$

where  $\hat{T}_E$  and  $\hat{T}_N$  are operators representing, respectively, the total electronic and nuclear kinetic energies.  $\hat{V}_{NN}$  is the potential energy operator including electrostatic repulsion of all nuclei and  $\hat{V}_{EE}$  is a similar type of operator accounting for the repulsions of all electrons.

It is possible to simplify the solution of equation (2.3) by making an assumption which is explained classically in the following manner. Due to their relatively large masses, the motion of nuclei is much less rapid than that of the electrons. In a given instant, electron motion occurs as if the positions of the nuclei were fixed. It should, therefore, be possible to determine molecular properties by

calculating electron motions for fixed nuclear configurations.

This approximation is translated into quantum mechanical terms by assuming that, if the nuclei are in fixed positions (where  $\hat{V}_N = 0$  and  $\hat{V}_{NN} = \text{constant}$ ) there is a set of electronic eigenfunctions,  $\psi_E$ , such that

$$\hat{H}_E \psi_E = E_E \psi_E \quad (2.4)$$

where

$$\hat{H}_E = \hat{T}_E + \hat{V}_{EN} + \hat{V}_{EE}. \quad (2.5)$$

Born and Oppenheimer first showed that if  $\psi_E$  is only a slowly varying function of nuclear coordinates, the  $E_E$  can be thought of as being part of the potential field in which the nuclei move while  $\hat{V}_{NN}$  supplies the other part of it. The equation for nuclear motion is, therefore

$$(\hat{T}_N + \hat{V}_{NN} + \hat{E}_E) \psi_N = E \psi_N. \quad (2.6)$$

The eigenvalues obtained are the eigenvalues of  $\hat{H}$  in equation (2.3) and they are obtained by solving equation (2.4) over a range of values for the nuclear coordinates. Each  $E_E$  value is then used as a parameter in equation (2.6) in order to obtain the energies  $E$  and a set of wavefunctions,  $\psi_N$ , for the nuclear motion. Each electronic state of the molecule yields a different set of these functions and energies. The complete wavefunctions are obtained from

$$\psi = \psi_E \psi_N \quad (2.7)$$

where this product is referred to as the zero-order Born-Oppenheimer approximation. Spin and relativistic considerations are neglected,

but the approximation allows electronic wavefunctions of systems to be described independently of nuclear ones and it is valid as long as the electronic wavefunction is essentially independent of nuclear coordinates.

In the approximation previously discussed, it is possible to consider electronic, vibrational and rotational motions as being separate because of the different time frame involved with each type. The total wavefunction can be written approximately as

$$\psi = \psi_V \psi_r \psi_E \quad (2.8)$$

and the total energies can be written as the total of the different types of energies:

$$E = E_V + E_E + E_r . \quad (2.9)$$

## 2.6 CLASSIFICATION OF ELECTRONIC STATES

Electronic states are normally classified according to spin multiplicity and symmetry transformation properties of the electronic wavefunction.

Each electron has a spin of  $\frac{1}{2}$  and if the coupling of individual spins with orbital motion is small, the total of these spins is a resultant which is half integral for an odd number and integral for an even number of electrons.

Coupling of the total spin angular momentum with orbital angular momentum can cause the molecular electronic states to split into  $2S+1$  components,  $S$  being the total spin quantum number. The value  $2S+1$  is referred to as the spin multiplicity of the state and is written as a superscript before the symbol indicating the symmetry species to which

the electronic wavefunction for the state belongs.

When the spins of all electrons are paired  $S = 0$  and singlet states arise. If electrons are located in orbitals in such a way that two electrons in different orbitals have their spins parallel,  $S = 1$  and the resulting state is a triplet. Quartets, doublets, etc. can occur depending on the value of  $2S+1$ . Most aromatic molecules have singlet ground states.

In linear polyatomic molecules, there is an axially symmetric electrostatic field about the nuclei and the electronic angular momentum about the molecular axis is conserved. Consequently, the classification of electronic states can be derived from vector models.

In non-linear molecules where symmetry is lower, electronic angular momentum is not conserved. The explanation of this, in classical terms, is that there is an exchange of angular momentum of nuclei and electrons due to the motion of the electrons in the electrostatic nuclear field. If the classification of states for such molecules is to be more thorough than that afforded by the multiplicity specification, group theory must be used. The states are then classified according to the transformation properties of their space wavefunctions when the symmetry operation of the point group to which the molecule belongs are applied. Each possible electronic wavefunction is a basis for one of the irreducible representations of the molecular point group and has the same symmetry species as the irreducible representation for which it is a basis. It is assumed that the nuclei are fixed in their equilibrium positions but this discussion also holds for non-equilibrium

nuclear configurations as long as they have the same symmetry as the equilibrium one.

For toluene and benzyl radicals (point group  $C_{2v}$ ) the electronic wavefunctions form the bases of the irreducible representations of the point group  $C_{2v}$ . Each possible electron configuration corresponds to an irreducible representation and if the symmetries of the molecular orbitals which contain the electrons are known, their direct product gives the symmetry of the electronic state. It can be seen by looking up the  $C_{2v}$  point group in a character table that the wavefunctions for the different electronic states have the symmetry species  $A_1$ ,  $A_2$ ,  $B_1$  and  $B_2$ .

## 2.7 THEORY OF ELECTRONIC TRANSITIONS

Electronic transitions normally give rise to spectra appearing in the ultraviolet and visible regions of the spectrum. Under high resolution it is possible to discern the vibrational and rotational structures of electronic spectra of molecules in the gas phase but in the condensed phase, electronic spectra are usually broad.

The energy separation of electronic states is of the order  $10,000-100,000 \text{ cm}^{-1}$  while the separations of vibrational and rotational states are  $100-10,000 \text{ cm}^{-1}$  and  $0.1-100 \text{ cm}^{-1}$ , respectively.<sup>30</sup>

The probability of transition between an upper and lower electronic state, the states being denoted by  $\psi_e$  and  $\psi_{e''}$ , respectively, is proportional to the square of the transition moment integral which is given by

$$R_{e',e''} = \langle \psi_{e'} | M | \psi_{e''} \rangle \quad , \quad (2.10)$$

M being the dipole moment operator. The transition is allowed only if  $R_{e'e''}$  is non-zero and that condition will occur only if the product  $\Gamma_{\psi_{e'}} \otimes \Gamma_M \otimes \Gamma_{\psi_e}$  is totally symmetric for at least one component of M. It is assumed here that the states involved are non-degenerate and that the nuclei are fixed.

Since the nuclei of molecules are actually in motion, it is necessary to re-state the selection rule using eigenfunctions involving nuclear coordinates. Using the Born-Oppenheimer approximation, the total eigenfunction can be written as:

$$\psi_{ev} = \psi_e \psi_v = \psi_e(q, Q) \psi_v(Q). \quad (2.11)$$

Q denotes all nuclear coordinates and q, all electronic coordinates. Rotational motion is neglected. The finer interaction of electronic and vibrational motion is also neglected but the part of the interaction which is expressed by having  $\psi_e$  as a function of Q is retained.<sup>29</sup>

As before, the transition probability is proportional to the square of the transition moment, given by

$$R_{e'v'e''v''} = \langle \psi_{e'v'} | M | \psi_{e''v''} \rangle. \quad (2.12)$$

Let the dipole moment operator, M, be separated into electronic and nuclear parts:

$$M = M_e + M_N. \quad (2.13)$$

The equation

$$R_{e'v'e''v''} = R_{e'e''} \langle \psi_{v'} | \psi_{v''} \rangle \quad (2.14)$$

is arrived at by substituting (2.13) into (2.12) and simplifying.

$R_{e'e''}$  varies slightly with Q since the electronic wavefunction,  $\psi_e$ ,

contains nuclear as well as electronic coordinates. The transition between two states  $\psi_{e'}$  and  $\psi_{e''}$  is permitted if  $R_{e'e''}$  is non-zero. In the case of toluene and benzyl radical (point group  $C_{2v}$ ) electronic transitions from a totally symmetric singlet ground state,  $^1A_1$ , to singlet excited states of  $A_1$ ,  $B_1$  and  $B_2$  symmetries are permitted; for benzyl radical ( $C_{2v}$ ) transitions from the ground doublet state  $^2B_1$  to doublet excited states  $A_1$ ,  $A_2$  and  $B_1$  are symmetry allowed.

The intensity of transitions between the vibrational levels of the electronic states is governed by the magnitude of the overlap integral  $\langle \psi_{v'} | \psi_{v''} \rangle$  and the selection rule is that the direct product  $\Gamma_{\psi_{v'}} \otimes \Gamma_{\psi_{v''}}$  must be totally symmetric for the integral to be non-zero.  $\psi_{v'}$  and  $\psi_{v''}$  must therefore belong to the same irreducible representation. Hence, transitions can only occur between vibrational states belonging to the same symmetry species.

The vibrationless levels of the electronic states can always combine to give the 0,0 band if the transition is electronically allowed. In either electronic state, transitions can occur between states in which any number of quanta of a totally symmetric vibration are excited. That is,

$$\Delta V_s = V_{s'} - V_{s''} = 0, \pm 1, \pm 2, \pm 3, \dots \quad (2.15)$$

In the case of non-totally symmetric vibrations, however, only the changes

$$\Delta V_a = V_{a'} - V_{a''} = 0, \pm 2, \pm 4, \dots \quad (2.16)$$

can occur in the quantum number.

## 2.8 VIBRONIC COUPLING

The dependence of the electronic wavefunction upon nuclear

coordinates,  $Q$ , permits the interaction of electronic and vibrational motion in polyatomic molecules so that factoring of  $R_{e'v'e''v''}$  in the manner of equation (2.14) is no longer valid. When the nuclei are in a displaced position of a non-totally symmetric vibration, the molecule has lower symmetry than it would have in the equilibrium position and states which have different species in the equilibrium position can have the same species under reduced symmetry. The result is the mixing of the zeroth order vibrational levels of the electronic states involved and this type of interaction is known as the Herzberg-Teller effect. Therefore, transitions which were previously forbidden electronically, can occur between the perturbing states each of which has assumed properties of the others. The Herzberg-Teller theory<sup>33</sup> treats the change in nuclear coordinates as a perturbation in the electronic Hamiltonian since the potential energy term,  $\hat{V}_{EN}$ , and the operator,  $\hat{H}_E$ , vary with change of nuclear coordinates in higher approximation.

In principle, two electronic states of any species can perturb each other if suitable vibrations are excited. In fact, such perturbations are very weak unless the species of the two electronic states do not differ by more than the species of one of the normal vibrations. This condition may be written as:

$$\Gamma_{\psi_a} \otimes \Gamma_{\psi_b} = \Gamma_Q \quad (2.17)$$

where  $\psi_a$  is the perturbed state,  $\psi_b$  is the perturbing state and  $Q$  is the normal coordinate representative of the vibration causing the perturbation.<sup>29</sup>

## 2.9 THE FRANCK-CONDON PRINCIPLE

The shape and intensity of an electronic absorption or emission spectrum is governed by the relative intensities of the vibrational substructure of the electronic transition. The Franck-Condon principle provides an understanding of these relative intensities and it is based on the fact that an electronic transition occurs much more rapidly ( $10^{-15}$  sec) than oscillation of the nuclei ( $10^{-12}$  sec) so the nuclear configuration remains essentially the same immediately before and immediately after the electronic transition.

If the electronic transition moment is considered to be approximately constant and if the total wavefunction can be considered as being composed of vibrational, rotational and electronic components, the intensity of the transition is dependent upon the extent to which the eigenfunctions of the participating vibrational levels overlap. That is, the intensity of the transition is proportional to the square of the vibrational overlap integral. This integral is termed the Franck-Condon factor.

Within a given vibrational level the most probable nuclear configuration is dependent upon the square of the vibrational eigenfunction for that level. There is, therefore, a probability distribution as a function of  $r$  within the level. Thus, in the case of emission at low temperature, a number of transitions can originate in the zeroth vibrational level of the excited electronic state.

In the approximation of constant nuclear configuration during an electronic transition, the most probable transition would correspond to a vertical line on the potential energy diagram, as in Figures 2.2a , 2.2c .

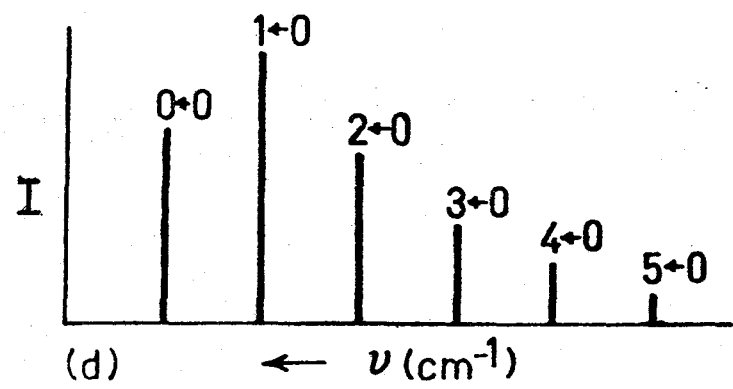
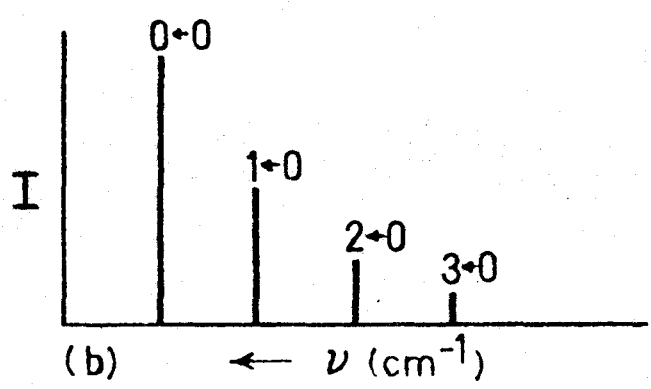
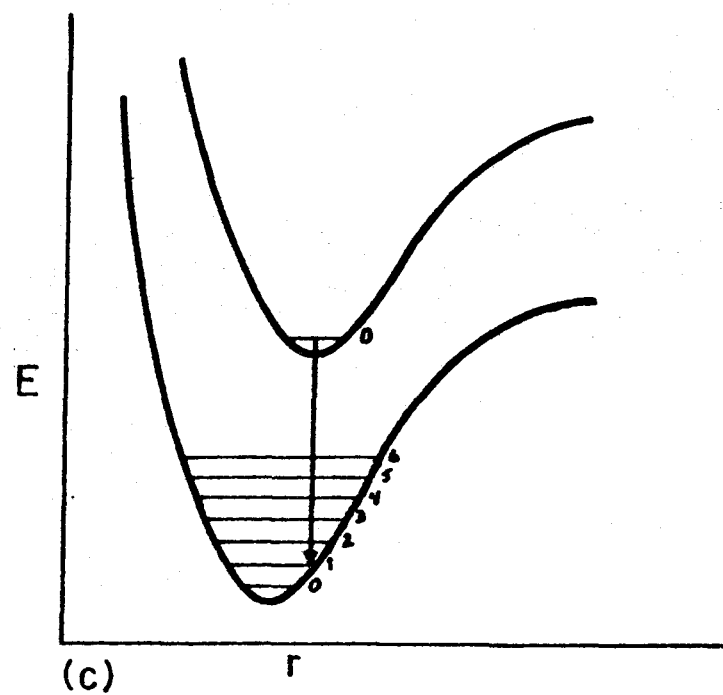
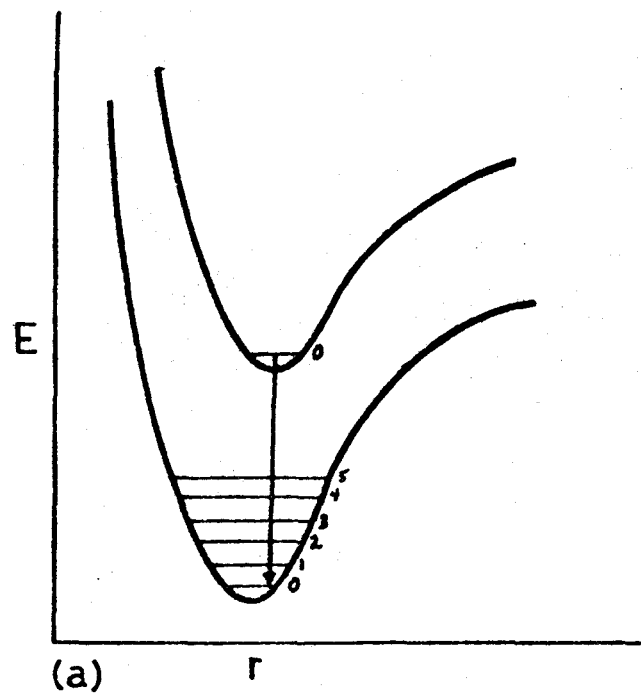


Figure 2.2 Franck-Condon potential curves for the ground and first excited states (a,c) and the resulting emission progression (b,d).

If the minima of the potential energy curves are not displaced with respect to each other, the 0,0 transition is the most intense and the intensity of the bands lessens gradually toward longer wavelengths, as shown in Figures 2.2a and 2.2b . This is the case for molecules which do not distort upon entering the excited electronic state. If the molecule does distort when so excited, the potential energy minima are displaced with respect to each other and the eigenfunctions of the zeroth vibrational level now overlaps more effectively with some other vibrational level of the ground state and the transition to this level will be most intense, as depicted in Figures 2.2c and 2.2d . There is also overlap with the eigenfunctions of a larger number of ground state vibrational levels so the spectral progressions involved are longer. Therefore, information concerning the excited state geometry of a molecule can be deduced from the most prominent vibrational progressions.

## 2.10 FLUORESCENCE AND PHOSPHORESCENCE

After a molecule has become excited due to absorption of radiation, the extra energy can be lost through various radiative and non-radiative processes. Figure 2.3 ,referred to as a Jablonski diagram, indicates the types of processes involved. Solid, vertical lines represent spin allowed absorption and emission transitions while dashed vertical lines indicate spin forbidden absorption and emission. Horizontal dashed arrows represent intersystem crossing, while wavy, vertical lines indicate vibrational relaxation.

If a molecule is excited into one of the higher excited states of the singlet manifold,  $S_1$ , the energy can be degraded by internal

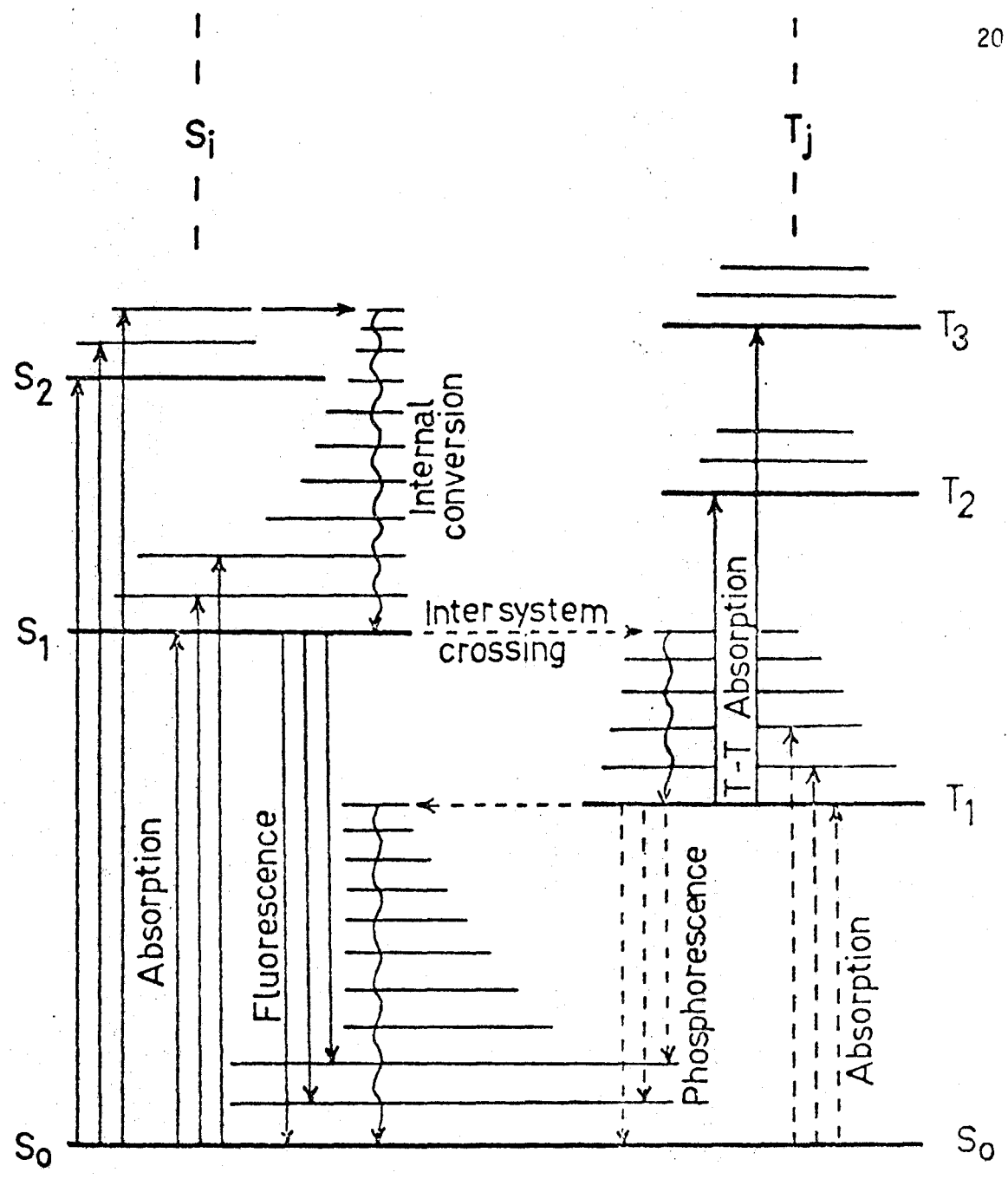


Figure 2.3 Schematic view of energy levels with possible absorption transitions and different types of mechanisms for intramolecular loss of energy.

conversion and vibrational relaxation. Internal conversion is defined as a non-radiative passage between electronic states of the same multiplicity. When the molecule undergoes internal conversion from  $S_i$  to  $S_1$  it can still be vibrationally excited within  $S_1$  and this excess vibrational energy is removed by the intermolecular process of vibrational relaxation so that, relative to the minimum of the  $S_1$  potential energy surface, a thermally equilibrated collection of  $S_1$  molecules is produced. In fact, emission from excited states above the zeroth vibrational level of  $S_1$  is seldom observed with molecules in rigid hydrocarbon glasses or polycrystalline matrices at 77°K. This is also the case for the triplet manifold. It is a general rule, known as Kasha's Rule,<sup>34</sup> that emission occurs from the  $S_1$  or  $T_1$  state, and not from higher excited states.

A molecule in the  $S_1$  state can undergo one of several possible processes:

- (i) Fluorescence, which is the radiative passage between states of the same multiplicity;
- (ii) Internal conversion and vibrational relaxation from  $S_1$  to  $S_0$ ;
- (iii) Intersystem crossing from  $S_1$  to  $T_1$  which is defined as the non-emissive passage between two states of different multiplicity.

If process (iii) occurs, vibrational relaxation then follows so the molecule is in the lowest vibrational level of the  $T_1$  state and one of the following processes happens:

- (i) Phosphorescence, which is the radiative passage between

- states of different multiplicity ( $T_1 \rightarrow S_0$  in this study);
- (ii)  $T_1 \rightsquigarrow S_0$  intersystem crossing, followed by vibrational relaxation within  $S_0$ .

Virtually all phosphorescence spectra are due to efficient intersystem crossing since singlet-triplet absorption is forbidden and  $T_1$  must be populated in some other manner. If the  $T_1 \rightsquigarrow S_0$  process was of comparable efficiency, phosphorescence would be observed only in rare cases. The disparity in the  $S_1 \rightsquigarrow T_1$  and  $T_1 \rightsquigarrow S_0$  rate constants can be as large as  $10^9$  and several workers have offered explanations for it. Kasha<sup>35</sup> proposed that the probability of  $S_1 \rightsquigarrow T_1$  increased as the energy difference between  $S_1$  and  $T_1$  decreased. Robinson<sup>36,37,38</sup> formulated a theory which embodies the idea of the intersystem rate constant  $k_{isc}$  for  $T_1 \rightsquigarrow S_0$  being very sensitive to the energy gap  $T_1-S_0$ . The sensitivity to the energy gap is contained in the overlap integrals of the two states between which energy is being non-radiatively transferred. The sensitivity of  $k_{isc}$  should be common to both intersystem crossing and internal conversion, and should be independent of spin reorientation processes.

Although intersystem crossing and direct absorption involving states of different multiplicity are both spin forbidden, their probabilities of occurrence are not equal. Spin orbit coupling is inversely proportional to the energy differences between the triplet and singlet states concerned. When the  $T_1-S_1$  energy differences ( $\sim 3000-9000 \text{ cm}^{-1}$ ) are considered, the probability for intersystem crossing should be larger than that for direct transition between the ground singlet and lowest triplet state. The  $S_1$  to  $T_1$  intersystem crossing process is slow compared

to the  $S_1$  and  $S_0$  fluorescence, but it competes well enough to populate the triplet state. See Table 2.3 where the processes and their rate constants are listed.

The degree to which the spin forbiddenness of singlet-triplet transitions is relaxed depends upon the magnitude of the interaction between the magnetic dipole generated by spin motion of the electron and that produced by its orbital motion. Such spin-orbit coupling, as the interaction is termed, causes the introduction of triplet character into singlet states and vice-versa.

In summary, the spectra which are obtained are the result of the collection of transitions from the zeroth vibrational level of the excited state. If the upper state is singlet, the spectra obtained are fluorescence and if the upper electronic state is a triplet, the spectra are termed phosphorescence spectra.

Molecular distortions of the singlet and triplet can be studied by examination of the vibrational structure of the relevant electronic transition.

## 2.11 CHARACTERISTICS OF POLYCRYSTALLINE MATRICES

In gas phase spectroscopy, emission from a higher vibrational level which has previously taken part in an absorption process frequently occurs. This phenomenon is termed resonance fluorescence and according to Kasha's rule does not occur in solid solutions at low temperatures. Kasha's rule also eliminates "hot bands" from consideration since no transitions having energy greater than that of the 0,0 can occur. The spectra obtained at low temperature using solid solutions are, therefore, much less complicated than their gas phase counterparts.

TABLE 2.3

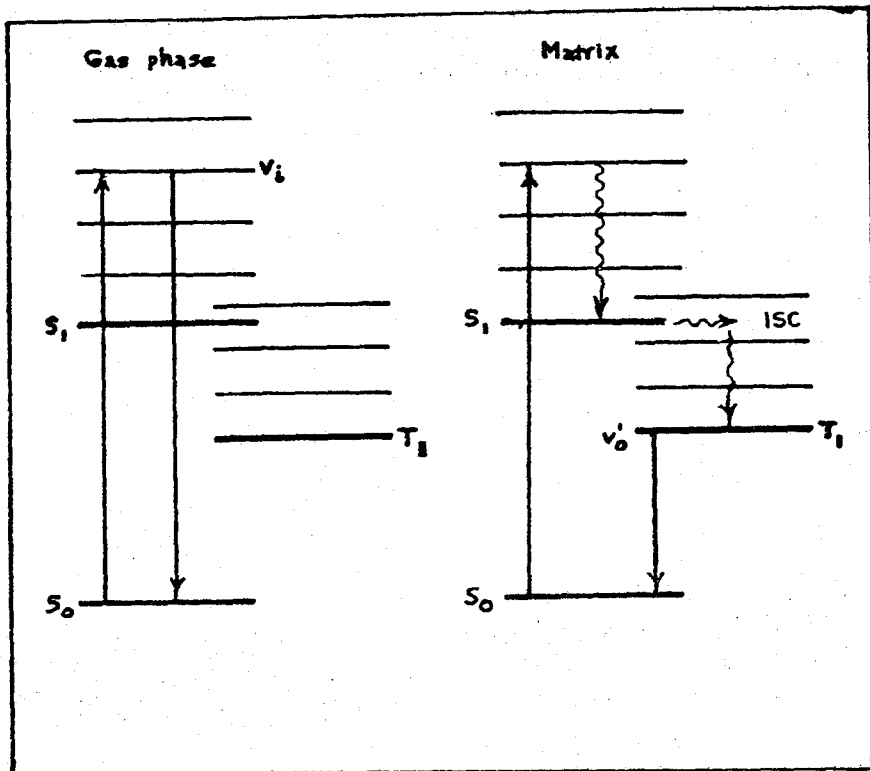
Rate Constants for Radiative and Non-Radiative Processes in Rigid Media  
at 77°K.

| Process  | Rate Constant (sec <sup>-1</sup> ) |
|--|------------------------------------|
| Absorption, $S \rightarrow S_1$                      | $10^{15}-10^{16}$                  |
| Internal Conversion, $S_2 \rightsquigarrow S_1$      | $> 10^{12}$                        |
| Vibrational Relaxation within $S_1$ , $T_1$ or $S_0$ | $> 10^{12}$                        |
| Fluorescence, $S_1 \rightarrow S_0$                  | $10^6-10^9$                        |
| Internal Conversion, $S_1 \rightsquigarrow S_0$      | $10^6-10^{12}$                     |
| Intersystem Crossing, $S_1 \rightsquigarrow T_1$     | $10^4-10^{12}$                     |
| Phosphorescence, $T_1 \rightarrow S_0$               | $10^{-2}-10^4$                     |
| Intersystem Crossing, $T_1 \rightsquigarrow S_0$     | $10^{-1}-10^5$                     |

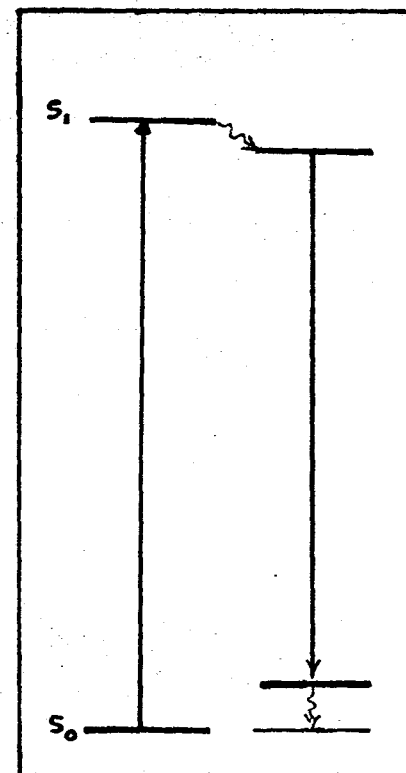
The solvent-solute system can be thought of as being an infinitely dilute cold gas.<sup>39</sup> In such a system, the guest molecules are isolated from each other so there is little guest-guest interaction. The solvent is considered to be virtually inert and host-guest interaction is minimized. Spectra obtained from such guests are characteristic of the free molecule because there is little interaction between the molecule and the environment to cause distortion of the energy level system. Absorption or emission of the host does not occur because the energy levels of such molecules are well above those of the guest. Both polycrystalline matrices and organic-glass solvents manifest these solvent characteristics.

Typically, the wavelength of electronic and vibrational transitions changes by less than one percent on going from the gas phase to the solid. This slight shift arises from the fact that the excited state of the guest interacts with the host system to a different extent than in the case with the guest ground state, as shown in Figures 2.4a and 2.4b. The shift is an indicator of the relative difference in interaction energy on going from one phase to the other. The wavelength of the transition may be blue or red shifted depending on the relative magnitudes of the interactions involved.

Usually, the 0,0 transition of fluorescence does not coincide with the 0,0 of absorption in the solid phase. This is expected because each solute molecule is rigidly surrounded by solvent molecules. Upon absorption of light, the solute molecule is in an unstable excited state configuration relative to the surrounding solvent molecules. However, the solute molecule usually has time to achieve a stable, equilibrium



(a)



(b)

Figure 2.4a Comparison of gas phase and matrix emission.  
 2.4b Difference of 0,0 energies for absorption and emission.

configuration before emitting. When emission has occurred, the guest molecule will be in an unstable configuration with regard to the ground state and will undergo relaxation. Thus, the 0,0 transition of emission is of lower energy than the absorption one in solid phase spectra.

When a solvent whose molecular dimensions closely match those of the solute is chosen and a polycrystalline matrix is formed, sharp spectra are often obtained. This phenomenon is called the Shpol'skii effect.<sup>39</sup> When solute and solvent are not matched in that manner, poorly resolved spectra usually result. Careful choice of solvent and the use of polycrystalline samples can lead to much sharper spectra being obtained.

It occasionally happens that spectra obtained using Shpol'skii solvents exhibit peak splitting which is due to multiple site emission. If cyclohexane, for example, is frozen too rapidly, two crystalline modifications of the solvent will appear in the same sample and two similar spectra corresponding to the emission of the solute from the cubic and monoclinic environments will be obtained. The separation of corresponding peaks can be as much as 100 cm.<sup>40</sup> Slow cooling of the sample eliminates this problem by allowing cyclohexane to solidify in monoclinic form only.

Splitting of spectral peaks can also be caused by emission from guest molecules having several preferred orientations in the sample.<sup>41</sup> Again, cooling the sample slowly is the best preventative measure.

## CHAPTER III

### EXPERIMENTAL

#### 3.1 CHEMICALS

$C_6H_5CH_3$  of scintillation quality was purchased commercially from Matheson, Coleman and Bell. It was vacuum distilled before use but the emission spectra obtained before and after this distillation were virtually identical.

$C_6D_5CH_3$  of greater than 99% isotopic purity was obtained from Merck, Sharp and Dohme of Canada. Vacuum distillation of it was carried out but this was found to have been unnecessary since emission spectra taken before and after the distillation were identical.

$C_6H_5CD_3$  was bought from Stohler Isotope Chemicals. It was also more than 99% isotopically pure and was used as received.

$C_6D_5CH_3$  was prepared according to the method of Werstiuk and Kadai<sup>42</sup> involving acid catalyzed exchange of aromatic protons by deuterium at high temperature.

The o, m and p-deuterotoluenes were obtained from the corresponding mono-brominated toluenes (British Drug Houses, Laboratory Reagent) by preparing the corresponding Grignard reagent and hydrolyzing it with  $D_2O$ . The product was then purified by distillation using a Vigreux column.

The deuterated derivatives were all checked for isotopic purity

by Carbon-13 magnetic resonance.<sup>43</sup> Toluene-d<sub>8</sub>, toluene  $\alpha$ -d<sub>3</sub> and toluene-d<sub>5</sub> were checked by this method and they were found to have deuterium incorporations in the desired positions in excess of 95%.

The ortho-, meta- and para-monodeuterated toluenes had deuterium incorporations of 92%, 92% and 82%, respectively, as estimated by Carbon-13 n.m.r.

The benzyl radicals were produced from the analogous toluenes in  $10^{-2}$ - $10^{-3}$  M solutions by 15-20 minutes irradiation with 270 nm. light provided by an Osram 450 watt Xe lamp. Samples which were prepared in this way and kept frozen in liquid nitrogen gave reproducible spectra as long as thirty-six hours after preparation.

### 3.2 SOLVENTS

Methylcyclohexane, cyclohexane, hexane and heptane were Matheson, Coleman and Bell "spectroquality" chemicals and were used without further purification.

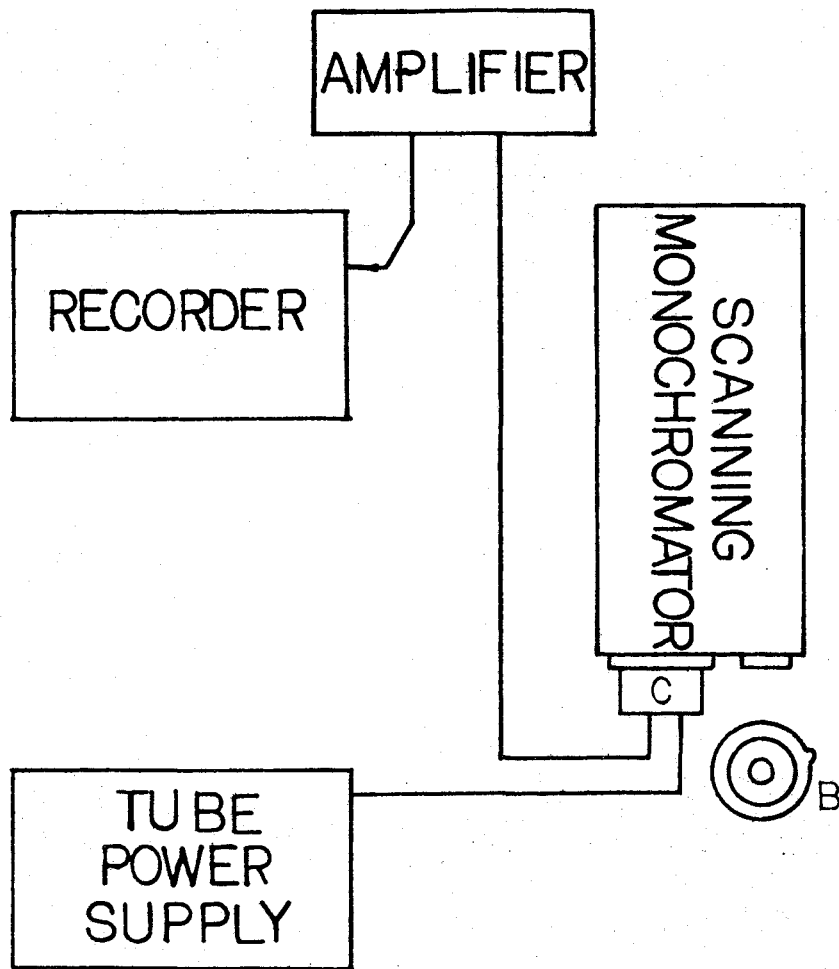
3-Methylpentane (3-MP) was pure grade Phillip 66 and was passed through a Linde 10X molecular sieve before being used.

These materials all failed to show detectable luminescence under the conditions employed in obtaining spectra.

### 3.3 APPARATUS

Figure 3.1 provides a schematic illustration of the apparatus used to obtain the emission spectra.

The exciting light was obtained from a low pressure mercury lamp or from a high pressure 450 watt xenon lamp powered by a D.C. regulated Universal lamp power supply Model #C-72-50 from Oriel Optics



A LENSES

B DEWAR AND SAMPLE

c PHOTOMULTIPLIER TUBE

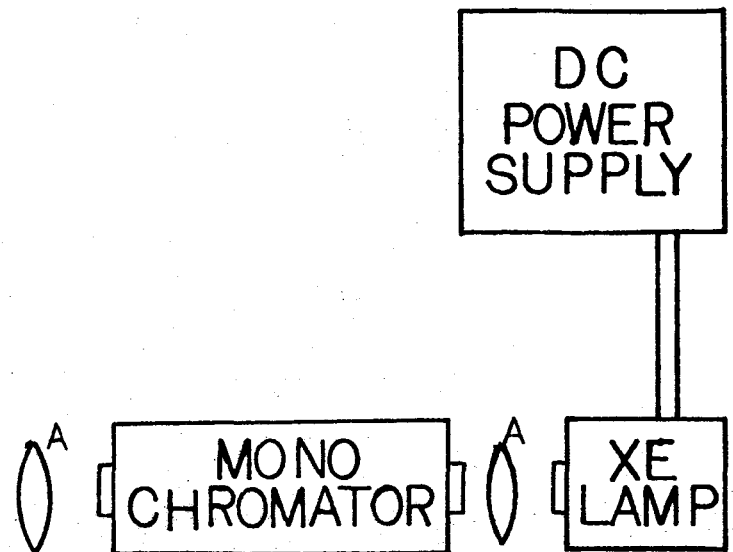


FIG. 3.1 APPARATUS FOR EMISSION EXPERIMENTS

BLOCK  
DIAGRAM

Corporation. Most of the intensity of the mercury lamp emission was concentrated at 253.7 nm and it was this wavelength which was used to excite toluene. The 450 watt xenon lamp has a white emission so it was necessary to pass the light from it through a Jarrell-Ash 0.25 meter Ebert monochromator whose grating, blazed at 300 nm, has 2360 grooves/mm. This light source was used in obtaining benzyl radical spectra, the excitation wavelength being 317 nm.

The exciting light was then focussed by quartz lenses on the sample within an 11 mm O.D. quartz tube which was submerged in a partially silvered dewar containing liquid nitrogen.

The light emitted by the sample was passed through a 0.5 meter Jarrell-Ash scanning monochromator whose grating, blazed at 400 nm, has 1180 grooves/mm. This monochromator was mounted at right angles to the direction of the exciting light and was equipped with an RCA 8575 photomultiplier tube powered by a Power Design Model HV1544 power supply.

The photomultiplier output signal was then amplified in one of two ways:

- (1) by a Keithley Model 610C electrometer;
- (2) by an Ortec Model 454 Timing Filter Amplifier used with an Ortec photon counting system consisting of a Model 421 Integral Discriminator, a Model 441 Ratemeter, and a 9201 Photomultiplier base.

The spectra were obtained using  $10^{-2}$ - $10^{-4}$  M solutions and were uncorrected for instrumental response. The estimated accuracy of the luminescence spectra is  $\pm 1\text{Å}$ . The spectra were calibrated using mercury emission lines.

## CHAPTER IV

### RESULTS AND DISCUSSION

At 77°K, the Boltzmann factor,  $kT$ , is approximately  $50 \text{ cm}^{-1}$ . This value is somewhat smaller than the spacing between vibrational levels so there is little thermal population of higher vibrational levels in the excited states. Consequently, transitions occur from the zeroth vibrational level of  $S_1$  or  $T_1$  and terminate at some vibrational level in the ground state.

The ground state fundamentals used in this work are portrayed schematically in Figure 4.1, where they are designated by Whiffen's notation for monosubstituted benzenes. The complete set of toluene fundamental frequencies is given in Table 4.1, where the Whiffen,<sup>44</sup> Wilson<sup>45</sup> and Herzberg<sup>29</sup> designations are shown.

The resolution of the toluene fluorescence and phosphorescence spectra and benzyl radical fluorescence spectra was rather poor with most solvents used (such as hexane or cyclopentane) although the main features of the spectra were similar from solvent to solvent at 77°K. Polycrystalline methylcyclohexane was the solvent used in obtaining the spectra analyzed in this study, since well resolved spectra were recorded for the fluorescence and phosphorescence of toluene and for the fluorescence of benzyl radical at 77°K. In cases where the methylcyclohexane solvent was present as a glass or cracked glass, the overall appearance of a spectrum was the same as observed with the polycrystalline matrix but resolution was much poorer.

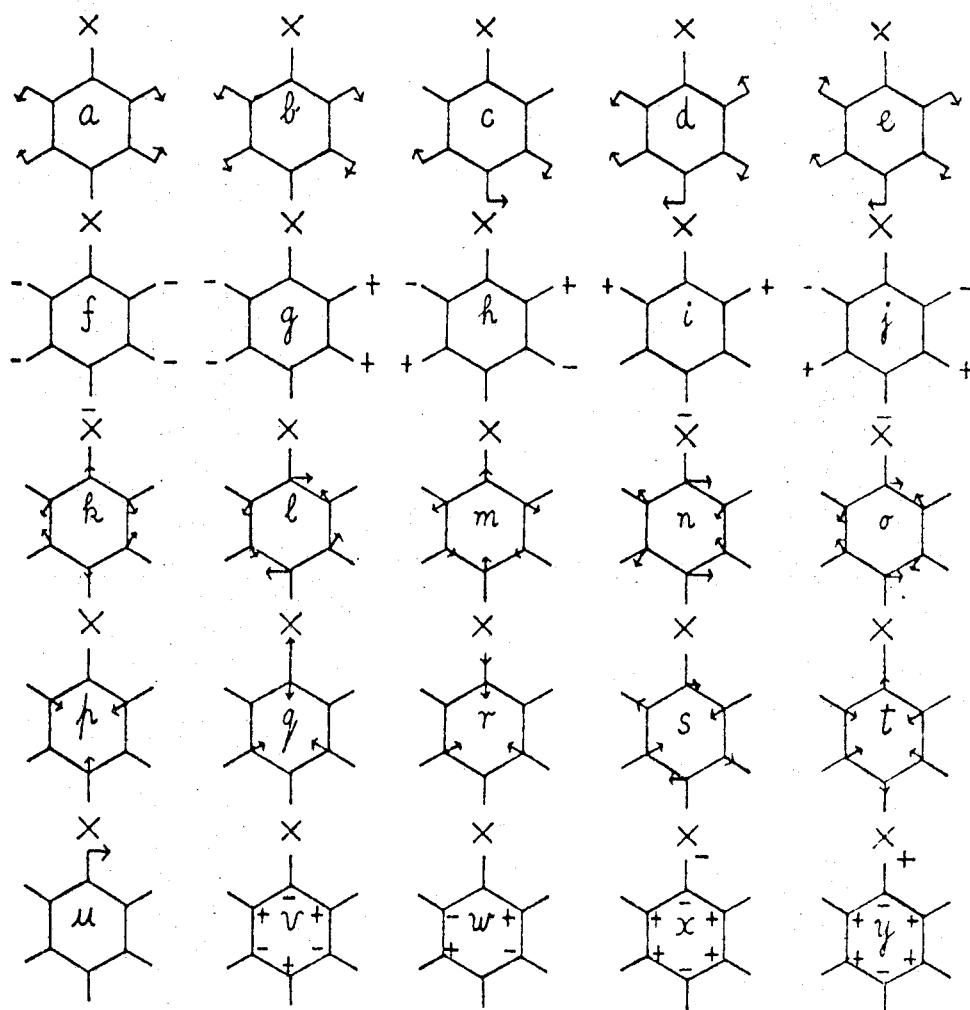


Figure 4.1 Schematic illustrations of some vibrational modes of mono-substituted benzenes.

TABLE 4.1

Ground State Fundamentals in Toluene and Some of its Deuterated Derivatives.

| Designation <sup>a</sup> | Symmetry                     | Description        | Frequency (cm <sup>-1</sup> ) |                   |                   |                 |                   |                 |                   |                   |
|--------------------------|------------------------------|--------------------|-------------------------------|-------------------|-------------------|-----------------|-------------------|-----------------|-------------------|-------------------|
|                          |                              |                    | C <sub>2v</sub>               | C <sub>s</sub>    | of h8 mode        | h8 <sup>b</sup> | α-d3 <sup>b</sup> | d5 <sup>c</sup> | d8 <sup>b</sup>   | p-d1 <sup>b</sup> |
| v <sub>1</sub>           | 7a                           | a <sub>1</sub> a'  | νC-H                          | 3085 <sup>d</sup> | 3087 <sup>d</sup> | 2300            |                   | 2262            | 2266              | 2985              |
| v <sub>2</sub>           | 20a                          | a <sub>1</sub> a'  | νC-H                          | 3063              | 3063              | 2285            | 2293              | 3079            | 3087              | 2259              |
| v <sub>3</sub>           | 2                            | a <sub>1</sub> a'  | νC-H                          | 3055              | 3056              | 2271            | 2286              | 3054            | 3056              | 3044              |
| v <sub>4</sub>           | ν <sub>s</sub>               | a <sub>1</sub> a'  | νCH <sub>3</sub>              | 2921              | 2130              | 2920            | 2121              | 2898            | 2923              | 2920              |
| k v <sub>5</sub>         | 8a                           | a <sub>1</sub> a'  | νC-C                          | 1605              | 1606              | 1569            | 1583              | 1601            | 1600              | 1600              |
| m v <sub>6</sub>         | 19a                          | a <sub>1</sub> a'  | νC-C                          | 1494              | 1495              | 1390            | 1388              | 1491            | 1482              | 1477              |
| v <sub>7</sub>           | δ <sub>s</sub>               | a <sub>1</sub> a'  | δCH <sub>3</sub>              | 1379              | 1045              | 1378            | 1041              | 1380            | 1378              | 1380              |
| q v <sub>8</sub>         | 13                           | a <sub>1</sub> a'  | X-sens(νC-Me)                 | 1208              | 1225              | 1144            | 1180              | 1211            | 1205              | 1203              |
| a v <sub>9</sub>         | 9a                           | a <sub>1</sub> a'  | βC-H                          | 1175              | 1180              | 871             | 880               | 1179            | 1155 <sup>e</sup> | 1156              |
| b v <sub>10</sub>        | 18a                          | a <sub>1</sub> a'  | βC-H                          | 1030              | 1026              | 842             | 840               | 1029            | 1025              | 1033              |
| p v <sub>11</sub>        | 12                           | a <sub>1</sub> a'  | Ring                          | 1003              | 1003              | 961             | 961               | 986             | 1002              | 991               |
| r v <sub>12</sub>        | 1                            | a <sub>1</sub> a'  | X-sens(αC-C-C)                | 784               | 758               | 741             | 717               | 785             | 763               | 788               |
| t v <sub>13</sub>        | 6a                           | a <sub>1</sub> a'  | X-sens(αC-C-C)                | 521               | 498               | 507             | 490               | 517             | 520               | 525               |
| h v <sub>14</sub>        | 17a                          | a <sub>2</sub> a'' | γC-H                          | 964               | 966               | 790             |                   | 917             | 889               | 914               |
| g v <sub>15</sub>        | 10a                          | a <sub>2</sub> a'' | γC-H                          | 843               | 840               | 660             |                   |                 | 836               | 834               |
| w v <sub>16</sub>        | 16a                          | a <sub>2</sub> a'' | φC-C                          | 408               | 361               | 355             | 349               | 411             | 389               | 398               |
| v <sub>17</sub>          | ν <sub>a</sub> <sup>''</sup> | b <sub>1</sub> a'' | νCH <sub>3</sub>              | 2979              | 2230              | 2970            | 2241              | 2959            | 2976              | 2975              |
| v <sub>18</sub>          | δ <sub>a</sub> <sup>''</sup> | b <sub>1</sub> a'' | δCH <sub>3</sub>              | 1460              | 1050              | 1448            | 1049              | 1450            | 1462              | 1465              |
| v <sub>19</sub>          | r <sup>''</sup>              | b <sub>1</sub> a'' | rCH <sub>3</sub>              | 1040              | 845               | 1035            | 770               | 1040            | 1046              | 1040              |
| j v <sub>20</sub>        | 5                            | b <sub>1</sub> a'' | γC-H                          | 978               | 980               | 816             | 785               | 947             | 917               | 943               |
| i v <sub>21</sub>        | 10b                          | b <sub>1</sub> a'' | γC-H                          | 893               | 917               | 735             | 735               | 834             | 800               | 765               |
| f v <sub>22</sub>        | 11                           | b <sub>1</sub> a'' | γC-H                          | 728               | 709               | 621             | 541               | 608             | 646               | 636               |
| v v <sub>23</sub>        | 4                            | b <sub>1</sub> a'' | φC-C                          | 695               | 698               | 551             |                   | 710             | 695               | 720               |
| x v <sub>24</sub>        | 16b                          | b <sub>1</sub> a'' | X-sens(φC-C)                  | 464               | 446               | 413             | 390               | 453             | 453               | 461               |
| y v <sub>25</sub>        | 17b                          | b <sub>1</sub> a'' | X-sens(γC-Me)                 | 217               | 206               | 208             | 197               | 208             | 215               | 218               |

TABLE 4.1 (Continued)

| Designation       | a               | Symmetry        |                | Description<br>of h8 mode | Frequency (cm <sup>-1</sup> ) |                   |                 |                 |                   |                   |                   |
|-------------------|-----------------|-----------------|----------------|---------------------------|-------------------------------|-------------------|-----------------|-----------------|-------------------|-------------------|-------------------|
|                   |                 | C <sub>2v</sub> | C <sub>s</sub> |                           | h8 <sup>b</sup>               | α-d3 <sup>b</sup> | d5 <sup>c</sup> | d8 <sup>b</sup> | p-d1 <sup>b</sup> | m-d1 <sup>b</sup> | o-d1 <sup>b</sup> |
| v <sub>26</sub>   | 7b              | b <sub>2</sub>  | a'             | νC-H                      | 3039                          | 3038              | 2255            | 2260            | 3042              | 3033              | 3067              |
| v <sub>27</sub>   | 20b             | b <sub>2</sub>  | a'             | νC-H                      | 3029                          | 3029              | 2265            | 2250            | 3024              | 3020              | 3019              |
| v <sub>28</sub>   | v' <sub>a</sub> | b <sub>2</sub>  | a'             | νCH <sub>3</sub>          | 2952                          | 2209              | 2948            | 2211            | 2959              | 2948              | 2950              |
| l v <sub>29</sub> | 8b              | b <sub>2</sub>  | a'             | νC-C                      | 1586                          | 1586              | 1556            | 1570            | 1579              | 1582              | 1590              |
| n v <sub>30</sub> | 19b             | b <sub>2</sub>  | a'             | νC-C                      | 1468                          | 1448              | 1322            | 1332            | 1420              | 1450              | 1450              |
| v <sub>31</sub>   | δ' <sub>a</sub> | b <sub>2</sub>  | a'             | δCH <sub>3</sub>          | 1460                          | 1050              | 1448            | 1049            | 1450              | 1462              | 1464              |
| e v <sub>32</sub> | 3               | b <sub>2</sub>  | a'             | βC-H                      | 1331                          | 1300              | 1071            | 972             | 1317              | 1290              | 1284              |
| o v <sub>33</sub> | 14              | b <sub>2</sub>  | a'             | νC-C                      | 1318                          | 1261              | 1284            | 1270            | 1319              | 1315              | 1298              |
| c v <sub>34</sub> | 9b              | b <sub>2</sub>  | a'             | βC-H                      | 1154                          | 1154              | 838             | 869             | 866               | 1165              | 1126              |
| d v <sub>35</sub> | 18b             | b <sub>2</sub>  | a'             | βC-H                      | 1080                          | 1073              | 816             | 819             | 1105              | 1100              | 867               |
| v <sub>36</sub>   | r'              | b <sub>2</sub>  | a'             | rCH <sub>3</sub>          | 1040                          | 845               | 1035            | 770             | 1040              | 1046              | 1040              |
| s v <sub>37</sub> | 6b              | b <sub>2</sub>  | a'             | αC-C-C                    | 623                           | 623               | 597             | 605             | 616               | 618               | 619               |
| u v <sub>38</sub> | 15              | b <sub>2</sub>  | a'             | X-sens(βC-Me)             | 344                           | 307               | 335             | 298             | 338               | 344               | 348               |

a Designations of modes of those of Whiffen,<sup>44</sup> Herzberg<sup>29</sup> and Wilson,<sup>45</sup> respectively.

b From Varsanyi.<sup>46</sup>

c From Hitchcock and Laposa.<sup>47</sup>

d From Fuson et al.<sup>48</sup>

e From this work.

TABLE 4.2

## Description of the Benzene Ring and Ring-Substituent Vibrations of Toluene .

| Abbreviated Form     | Description  |
|----------------------|--|
| $\nu\text{C-H}$      | C-H stretching.  |
| $\beta\text{C-H}$    | C-H in-plane deformation.  |
| $\gamma\text{C-H}$   | C-H out-of-plane deformation.  |
| $\nu\text{C-C}$      | C-C stretching.  |
| $\alpha\text{C-C-C}$ | Ring in-plane deformation.   |
| $\phi\text{C-C}$     | Ring out-of-plane deformation.   |
| Ring                 | Ring breathing mode.   |
| $\nu\text{C-Me}$     | C-C stretching between benzene ring and substituent group.   |
| $\beta\text{C-Me}$   | C-C in-plane deformation between benzene ring and methyl group.  |
| $\gamma\text{C-Me}$  | C-C out-of-plane deformation between ring and methyl group.  |
| X-sens               | Substituent, X, sensitive vibrations in which X moves with substantial amplitude so that the frequencies are sensitive to the mass of X. |
| $\nu\text{CH}_3$     | Symmetric ( $\nu_s$ ) and antisymmetric ( $\nu_a', \nu_a''$ ). C-H stretching modes within the methyl group.                             |
| $\delta\text{CH}_3$  | Symmetric ( $\delta_s$ ) and antisymmetric ( $\delta_a', \delta_a''$ ) bending modes within the methyl group.                            |
| $r\text{CH}_3$       | Rocking movements the methyl group in the molecular plane ( $r'$ ) and out of the molecular plane ( $r''$ ).                             |

#### 4.1 VIBRATIONAL ANALYSIS OF PHOSPHORESCENCE OF TOLUENES

##### a. Toluene-h8

The phosphorescence spectrum of toluene is shown in Figure 4.2 and the vibrational analysis is presented in Table 4.3. Kanda and Shimada<sup>8</sup> observed the 0,0 transition of toluene phosphorescence at  $28,920 \text{ cm}^{-1}$ , using cyclohexane as solvent at  $77^\circ\text{K}$ , while Kanda and Sponer<sup>9</sup> who studied the triplet singlet emission of toluene crystals at  $4^\circ\text{K}$ , and of toluene in ether-isopentane-alcohol (EPA) solvent at  $77^\circ\text{K}$ , found the 0,0 transitions at  $28,789 \text{ cm}^{-1}$  and  $28,889 \text{ cm}^{-1}$ , respectively. With the exception of an out-of-plane  $b_1$  mode at  $440 \text{ cm}^{-1}$ , Kanda and Shimada observed no bands between the 0,0 transition and  $660 \text{ cm}^{-1}$ . With the EPA solvent, Kanda and Sponer observed no peaks in the low frequency region and those noticed by them in their study of toluene crystal at  $4^\circ\text{K}$  were assigned as lattice vibrations. Recently, Haaland and Nieman<sup>10</sup> studied toluene phosphorescence in a benzene matrix at  $4^\circ\text{K}$  and assigned the 0,0 transition as  $28,994 \text{ cm}^{-1}$  while observing peaks at  $228 \text{ cm}^{-1}$  and  $454 \text{ cm}^{-1}$  which were assigned as out-of-plane fundamentals. In addition, an out-of-plane fundamental was observed at  $475 \text{ cm}^{-1}$  along with two weaker bands which were assigned as  $0,2 \times 228$  and  $0,3 \times 228$ , respectively. The progression in  $228 \text{ cm}^{-1}$  was not observed in this work where methylcyclohexane was the solvent at  $77^\circ\text{K}$ . However, the 0,0 value obtained in this study was  $29,010 \text{ cm}^{-1}$  which is in very good agreement with that found when benzene was used as the matrix. Evans<sup>7</sup> also obtained a value of  $29,000 \text{ cm}^{-1}$  using oxygen perturbation, to effect singlet triplet absorption. The  $200 \text{ cm}^{-1}$  and  $445 \text{ cm}^{-1}$  modes, which were assigned as 0,y and 0,x, respectively, did not combine with the main progressions in the spectrum. The  $b_1$  mode  $\nu$  also

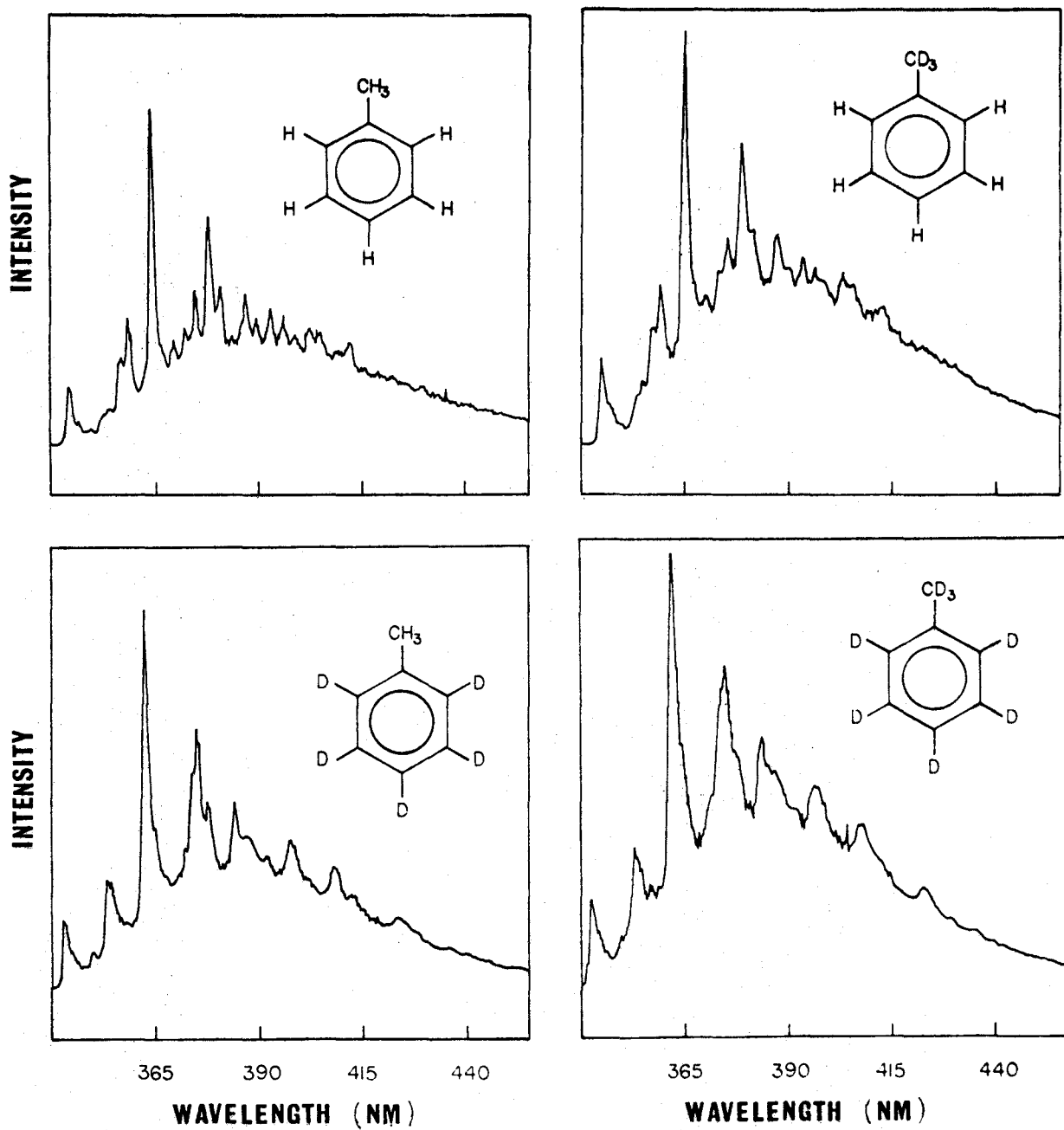


Figure 4.2 Phosphorescence spectra of (clockwise from upper left) toluene- $\text{h}_8$ , toluene- $\alpha$ - $\text{d}_3$ , toluene- $\text{d}_8$  and toluene- $\text{d}_5$ , all solutions  $10^{-3}\text{M}$  in methylcyclohexane matrices at  $77^\circ\text{K}$ .

TABLE 4.3

Vibrational Analyses of Phosphorescences of  $10^{-3}$  M  $C_6H_5CH_3$  and  $10^{-3}$  M  $C_6H_5CD_3$  in Polycrystalline Methylcyclohexane Matrices at 77°K.

| Toluene-h8          |                      | Toluene- $\alpha$ -d3 |             | Assignment <sup>a</sup> |
|---------------------|----------------------|-----------------------|-------------|-------------------------|
| $\nu$ ( $cm^{-1}$ ) | $\Delta\nu$          | $\nu$ ( $cm^{-1}$ )   | $\Delta\nu$ |                         |
| 29010               | 0                    | 29020                 | 0           | 0,0                     |
| 28810               | 200                  | 28835                 | 185         | 0,y                     |
| 28565               | 445                  | 28615                 | 405         | 0,x                     |
| 28315               | 695                  | 28335                 | 685 sh      | 0,v                     |
| 28210               | 800                  | 28210                 | 810         | 0,r                     |
| 28005               | 1005                 | 28010                 | 1010        | 0,p                     |
| 27845               | 1165                 | 27855                 | 1165        | 0,a                     |
| 27795               | 1215 sh <sup>b</sup> | 27795                 | 1225 sh     | 0,q                     |
| 27430               | 1580                 | 27435                 | 1585        | 0,l                     |
| 27415               | 1595 sh              | 27420                 | 1600 sh     | 0,k                     |
| 27220               | 1790 sh              | 27225                 | 1795 sh     | 0,p+r                   |
| 27000               | 2010                 | 27025                 | 2000        | 0,2xp                   |
| 26,830              | 2180                 | 26815                 | 2205        | 0,a+p                   |
| 26,640              | 2370                 | 26655                 | 2365        | 0,l+r;0,k+r             |
| 26625               | 2385                 |                       |             | 0,k+r                   |
| 26420               | 2590                 | 26435                 | 2585        | 0,l+p                   |
| 26390               | 2650 sh              | 26415                 | 2605 sh     | 0,k+p                   |
| 26225               | 2775                 | 26280                 | 2740        | 0,l+a                   |
| 26205               | 2805 sh              | 26240                 | 2780        | 0,k+a                   |
| 26010               | 3000                 |                       |             | 0,3xp                   |
| 25820               | 3190                 | 25835                 | 3185        | 0,k+l                   |
| 25800               | 3210 sh              | 25805                 | 3215 sh     | 0,2xk                   |
| 25635               | 3375                 | 25675                 | 3345        | 0,l+p+r;0,k+p+r         |
| 25415               | 3595                 | 25430                 | 3590        | 0,l+2xp;0,k+2xp         |
| 25220               | 3790                 | 25240                 | 3780        | 0,a+l+p;0,a+k+p         |
| 25040               | 3970                 | 25055                 | 3965        | 0,k+l+r;0,2xk+r         |
| 24845               | 4165                 | 24850                 | 4170        | 0,k+l+p;0,2xk+p         |
| 24675               | 4335                 | 24665                 | 4355        | 0,a+k+l;0,a+2xk         |

TABLE 4.3 (Continued)

| Toluene-h8            |             | Toluene- $\alpha$ -d3 |             | Assignment <sup>a</sup>    |
|-----------------------|-------------|-----------------------|-------------|----------------------------|
| $\nu(\text{cm}^{-1})$ | $\Delta\nu$ | $\nu(\text{cm}^{-1})$ | $\Delta\nu$ |                            |
| 24420                 | 4590        | 24420                 | 4600        | 0, $\ell$ +3xp;0,k+3xp     |
| 24250                 | 4760        | 24280                 | 4740        | 0,2xk+ $\ell$ ;0,3xk       |
| 24055                 | 4955        | 24205                 | 4925        | 0,k+ $\ell$ +p+r;0,2xk+p+r |
| 23845                 | 5165        | 23855                 | 5165        | 0,k+ $\ell$ +2xp;0,2xk+2xp |
| 23640                 | 5370        | 23675                 | 5345        | 0,a+k+ $\ell$ +p;0,a+2xk+p |
| 23465                 | 5545        |                       |             | 0,2xk+ $\ell$ +r;0,3xk+r   |
| 23255                 | 5755        | 23250                 | 5770        | 0,2xk+ $\ell$ +p;0,3xk+p   |
| 23085                 | 5925        | 23070                 | 5950        | 0,a+2xk+ $\ell$ ;0,a+3xk   |

<sup>a</sup> Designation of normal modes according to Whiffen.

<sup>b</sup> sh = shoulder

TABLE 4.4

Vibrational Analyses of Phosphorescences of  $10^{-3}$  M  $C_6D_5CH_3$  and  $10^{-3}$  M  $C_6D_5CD_3$  in Polycrystalline Methylcyclohexane Matrices at  $77^\circ K$ .

| Toluene-d5            |                     | Toluene-d8            |             | Assignment <sup>a</sup> |
|-----------------------|---------------------|-----------------------|-------------|-------------------------|
| $\nu(\text{cm}^{-1})$ | $\Delta\nu$         | $\nu(\text{cm}^{-1})$ | $\Delta\nu$ |                         |
| 29145                 | 0                   | 29145                 | 0           | 0,0                     |
| 28995                 | 150                 | 29010                 | 135         | 0,y                     |
| 28795                 | 350                 | 28820                 | 325         | 0,x                     |
| 28570                 | 575                 | 28565                 | 580         | 0,v                     |
| 28410                 | 735 sh <sup>b</sup> | 28410                 | 735 sh      | 0,r                     |
| 28290                 | 855                 | 28295                 | 850         | 0,b                     |
| 28225                 | 920                 | 28250                 | 895 sh      | 0,a                     |
| 28170                 | 975 sh              | 28170                 | 975 sh      | 0,p                     |
| 27995                 | 1150                | 27980                 | 1165        | 0,q                     |
| 27600                 | 1545                | 27610                 | 1535        | 0,l;0,k                 |
| 27440                 | 1705 sh             | 27450                 | 1695 sh     | 0,p+k                   |
| 27210                 | 1935 sh             | 27210                 | 1935 sh     | 0,2xp                   |
| 27005                 | 2140                | 26985                 | 2160 sh     | 0,p+q                   |
| 26855                 | 2290                | 26870                 | 2275 sh     | 0,l+r;0,k+r             |
| 26725                 | 2420                | 26740                 | 2405 sh     | 0,a+l;0,a+k             |
| 26645                 | 2500                | 26655                 | 2490        | 0,l+p;0,k+p             |
| 26455                 | 2690                | 26455                 | 2690 sh     | 0,2xp+r                 |
| 26035                 | 3110                | 26060                 | 3085        | 0,k+l;0,2xk             |
| 25820                 | 3325                | 25840                 | 3305        | 0,2xa+l;0,2xa+k         |
| 25510                 | 3635                | 25495                 | 3650        | 0,l+p+q;0,k+p+q         |
| 25330                 | 3815                | 25330                 | 3815        | 0,k+l+r;0,2xk+r         |
| 25145                 | 4000                | 25185                 | 3960        | 0,k+l+p;0,2xk+p         |
| 24905                 | 4240                |                       |             | 0,l+2xp+r;0,k+2xp+r     |
| 24500                 | 4645                | 24530                 | 4610        | 0,2xk+l;0,3xk           |
| 24295                 | 4850                |                       |             | 0,2xa+k+l;0,2xa+2xk     |
| 23655                 | 5490                | 23680                 | 5465        | 0,a+2xk+l;0,a+3xk       |

<sup>a</sup> Designation of normal modes follows Whiffen.

<sup>b</sup> sh = shoulder

appeared at  $695\text{ cm}^{-1}$  but was weak and rather broad. This assignment was made on the basis of the isotope shift upon perdeuteration since the value for the corresponding peak in toluene-d<sub>8</sub> is  $580\text{ cm}^{-1}$ .

The main features of the toluene-h<sub>8</sub> spectrum in methylcyclohexane solvent include the very intense band at  $1580\text{ cm}^{-1}$ , which is attributed to one quantum of a  $b_2$  vibration, the C-C stretching mode  $\ell$ . There appears a shoulder at  $1595\text{ cm}^{-1}$ . The shoulder is not sharp but is definitely present for all toluenes in this study at  $77^\circ\text{K}$  and is clearly present at  $4^\circ\text{K}$  in crystalline benzene. It is assigned as the  $a_1$  C-C stretching mode  $k$ . The  $1580\text{ cm}^{-1}$  band serves as a false origin and its shoulder combines with  $a_1$  modes  $r$ ,  $p$ ,  $a$  and  $k$  to account for the majority of the bands. No progressions in non-totally symmetric modes are observed. The bands  $0,2 \times \ell$  and  $0,3 \times \ell$  seem to be absent, as well as progressions in the low frequency out-of-plane  $b_1$  modes, as mentioned above. Mode  $p$  also forms a progression. No methyl modes seem to be present in the spectrum, neither for toluene-h<sub>8</sub> nor for any of its deuterated relatives.

b. Toluene- $\alpha$ -d<sub>3</sub>

The phosphorescence spectrum of toluene- $\alpha$ -d<sub>3</sub> is quite similar to that for toluene-h<sub>8</sub>. The  $0,0$  transition appears at  $29,020\text{ cm}^{-1}$  and the most intense peak in the spectrum is assigned as  $0,\ell$  with  $0,k$  appearing as a slight shoulder on this band. The  $a_1$  mode  $a$  appears as a band of medium intensity and the  $a_1$  modes  $r$ ,  $p$  and  $a$  appear in combinations with the progression in  $k$ . There is a progression in  $p$  but it is very weak and  $0,3 \times p$  does not appear. The phosphorescence spectrum of this mole-

cule is presented in Figure 4.2 and the vibrational analysis is given in Table 4.3.

c. Toluene-d8

The phosphorescence spectrum and vibrational analysis for toluene-d8 are given in Figure 4.2 and Table 4.4, respectively. The 0,0 transition was observed at  $29,145\text{ cm}^{-1}$  indicating that perdeuteration of toluene shifts this transition  $135\text{ cm}^{-1}$  to the blue. The totally symmetric mode a is again prominent but is shifted to  $850\text{ cm}^{-1}$ . This large isotope shift is expected for mode a when toluene is perdeuterated so that the assignment of the 0,a transition in toluene is substantiated. The presence of the  $a_1$  fundamental q which appears as a shoulder at  $1215\text{ cm}^{-1}$  in toluene-h8 is also affirmed since it appears in the toluene-d8 spectrum as a weak band at  $1165\text{ cm}^{-1}$ . As was the case with toluene-h8 and toluene- $\alpha$ -d3, the most intense band of the spectrum is due to the 0, $\ell$  transition and it appears at  $1535\text{ cm}^{-1}$  in toluene-d8. Modes a, p and r, the latter two of which shift to  $975$  and  $735\text{ cm}^{-1}$ , respectively, combine with the false origin  $\ell$  and the progression in k. Mode a also combines with the progression in k and there is a weak progression in p. The low frequency out-of-plane modes v, x and y are shifted quite dramatically with x moving from  $445\text{ cm}^{-1}$  to  $325\text{ cm}^{-1}$  and y from  $200$  to  $135\text{ cm}^{-1}$ . These shifts are as expected on the basis of infrared frequencies reported for toluene-d8. As was mentioned previously, the most intense band in the spectrum of toluene-h8 was due to 0, $\ell$  at  $1580\text{ cm}^{-1}$ . It was possible to resolve a shoulder at  $1595\text{ cm}^{-1}$  which was assigned as a quantum of the  $a_1$  mode k. According to infrared data (see Table 4.1), perdeuteration affects both

both transitions to the same extent, shifting them approximately  $30 \text{ cm}^{-1}$  to the blue. However, in the spectrum of toluene-d8 in methylcyclohexane, the two bands were so close together that they could not be resolved. Since the  $b_2$  mode  $\ell$  was found to be much more intense in the spectra of the monodeuterated toluenes, toluene-h8 and toluene- $\alpha$ -d3, the most intense band of the toluene-d8 and toluene-d5 spectra was assigned as 0,k also.

d. Toluene-d5

The phosphorescence spectrum of toluene-d5 is almost identical to that of toluene-d8, and the vibrational analysis presented for the latter is quite valid for toluene-d5 also. The only difference in the spectra of the two molecules is that the band at  $920 \text{ cm}^{-1}$  in toluene-d5 appears as a doublet with the lower frequency member being assigned as 0,b ( $850 \text{ cm}^{-1}$ ) while the  $920 \text{ cm}^{-1}$  component was assigned as a quantum of the  $a_1$  mode a. There is the usual intense band at  $1545 \text{ cm}^{-1}$  assigned as 0, $\ell$  and the fundamentals p, r and a combine with k. The 0,0 transition was observed at  $29,145 \text{ cm}^{-1}$ , this value being identical to that obtained for toluene-d8. The phosphorescence spectrum of toluene-d5 is presented in Figure 4.2 and the vibrational analysis is given in Table 4.4.

e. Para-Deuterated Toluene

The overall appearance of the phosphorescence spectrum of para-deuterated toluene is similar to that of toluene-h8. The vibrational analyses, as expected, are also similar for both molecules. Vibrational mode p involves the para position and it is shifted from  $1000 \text{ cm}^{-1}$  in toluene-h8 to  $985 \text{ cm}^{-1}$  in para-deuterated toluene. For this molecule, the 0,0 transition was assigned as  $29,020 \text{ cm}^{-1}$ . The

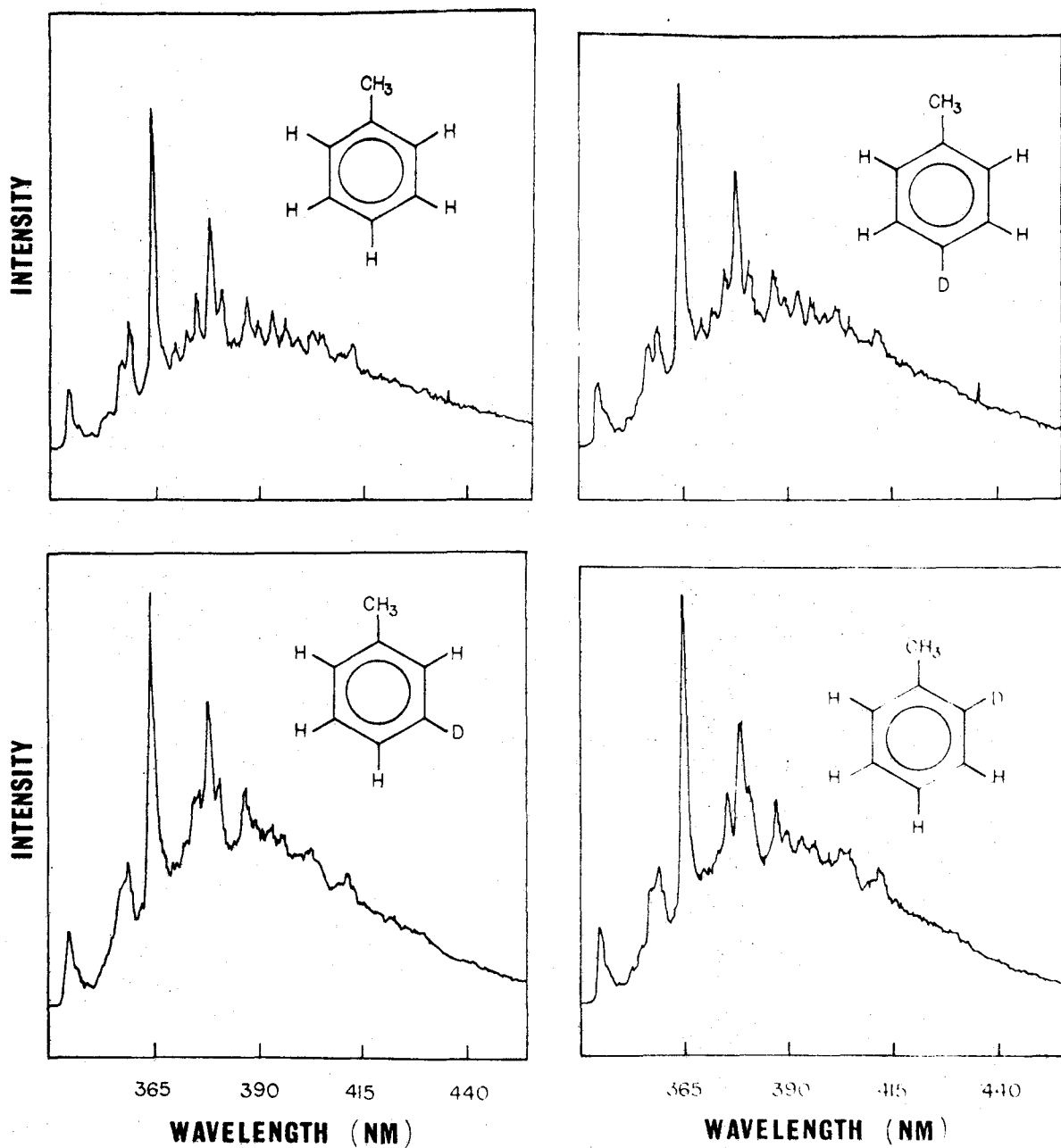


Figure 4.3 Phosphorescence spectra of (clockwise from upper left) toluene-h<sub>8</sub>, para, ortho and meta deuterated toluenes, all solutions 10<sup>-3</sup>M in methylcyclohexane matrices at 77°K.

TABLE 4.5

Vibrational Analyses of Phosphorescences of  $10^{-3}$  M para-D-C<sub>6</sub>H<sub>4</sub>CH<sub>3</sub>,  $10^{-3}$  M meta-D-C<sub>6</sub>H<sub>4</sub>CH<sub>3</sub>, and  $10^{-3}$  M ortho-D-C<sub>6</sub>H<sub>4</sub>CH<sub>3</sub> in Polycrystalline Methylcyclohexane Matrices at 77°K.

| para-d-Toluene        |                      | meta-d-Toluene        |             | ortho-d-Toluene       |             | Assignment <sup>a</sup> |
|-----------------------|----------------------|-----------------------|-------------|-----------------------|-------------|-------------------------|
| $\nu(\text{cm}^{-1})$ | $\Delta\nu$          | $\nu(\text{cm}^{-1})$ | $\Delta\nu$ | $\nu(\text{cm}^{-1})$ | $\Delta\nu$ |                         |
| 29020                 | 0                    | 29020                 | 0           | 29020                 | 0           | 0,0                     |
| 28850                 | 170                  | 28835                 | 185         | 28845                 | 175         | 0,y                     |
| 28615                 | 405                  | 28605                 | 415         | 28605                 | 415         | 0,x                     |
| 28435                 | 585                  | 28395                 | 625         | 28395                 | 625         | 0,f                     |
|                       |                      | 28345                 | 675         |                       |             | 0,v                     |
| 28210                 | 810                  | 28210                 | 810         | 28210                 | 810         | 0,r                     |
| 28035                 | 985                  | 28020                 | 1000        | 28020                 | 1000        | 0,p                     |
| 27955                 | 1165                 | 27865                 | 1155        | 27895                 | 1125        | 0,a                     |
| 27810                 | 1210 sh <sup>b</sup> | 27810                 | 1210        | 27810                 | 1210        | 0,q                     |
| 27450                 | 1570                 | 27450                 | 1570        | 27450                 | 1570        | 0,l                     |
| 27430                 | 1590 sh              | 27425                 | 1595 sh     | 27425                 | 1595 sh     | 0,k                     |
| 27065                 | 1955                 | 27020                 | 2000        | 27025                 | 1995        | 0,2xp                   |
| 26855                 | 2165                 | 26860                 | 2170        | 26890                 | 2130        | 0,a+p                   |
| 26665                 | 2355                 | 26665                 | 2355        | 26655                 | 2365        | 0,l+r;0,k+r             |
|                       |                      | 26590                 | 2430        |                       |             | 0,f+p+r                 |
| 26475                 | 2545                 | 26450                 | 2570        | 26450                 | 2570        | 0,l+p                   |
| 26450                 | 2570 sh              | 26420                 | 2600 sh     | 26425                 | 2595 sh     | 0,k+p                   |
| 26275                 | 2745                 | 26280                 | 2740        | 26335                 | 2685        | 0,l+a;0,k+a             |
| 26060                 | 2960                 | 26035                 | 2985        | 26010                 | 3010        | 0,3xp                   |
| 25875                 | 3145                 | 25865                 | 3155        | 25865                 | 3155        | 0,k+l                   |
|                       |                      | 25815                 | 3205 sh     | 25800                 | 3210 sh     | 0,2xk                   |
| 25705                 | 3315                 | 25685                 | 3335        | 25700                 | 3320        | 0,l+p+r;0,k+p+r         |
| 25485                 | 3535                 | 25445                 | 3575        | 25445                 | 3575        | 0,2xp+l;0,k+2xp         |
| 25290                 | 3730                 | 25255                 | 3765        | 25280                 | 3740        | 0,a+l+p;0,a+k+p         |
| 25055                 | 3965                 | 25055                 | 3965        | 25080                 | 3940        | 0,k+l+r;0,2xk+r         |
| 24895                 | 4125                 | 24845                 | 4175        | 24875                 | 4145        | 0,k+l+p;0,2xk+p         |
| 24675                 | 4345                 | 24710                 | 4310        | 24765                 | 4255        | 0,a+k+l;0,a+2xk         |

TABLE 4.5 (Continued)

| para-d-Toluene        |             | meta-d-toluene        |             | ortho-d-toluene       |             | Assignment <sup>a</sup> |
|-----------------------|-------------|-----------------------|-------------|-----------------------|-------------|-------------------------|
| $\nu(\text{cm}^{-1})$ | $\Delta\nu$ | $\nu(\text{cm}^{-1})$ | $\Delta\nu$ | $\nu(\text{cm}^{-1})$ | $\Delta\nu$ |                         |
|                       |             | 24400                 | 4620        |                       |             | $0,3xp+l;0,k+3xp$       |
| 24315                 | 4705        | 24295                 | 4725        | 24295                 | 4725        | $0,2xk+l;0,3xk$         |
| 23920                 | 5100        |                       |             |                       |             | $0,k+l+2xp;0,2xk+2xp$   |
| 23705                 | 5315        | 23725                 | 5295        | 23795                 | 5225        | $0,a+k+l+p;0,a+2xl+p$   |
|                       |             | 23485                 | 5535        |                       |             | $0,2xk+l+r;0,3xk+r$     |
| 23350                 | 5670        | 23255                 | 5755        | 23300                 | 5710        | $0,2xk+l+p;0,3xk+p$     |

<sup>a</sup> Designation of normal modes follows Whiffen.

<sup>b</sup> sh = shoulder

spectrum is depicted in Figure 4.3 and the vibrational analysis is presented in Table 4.5.

f. Meta-Deuterated Toluene

The vibrational analysis presented for meta deuterated toluene in Table 4.5 is almost identical to that for toluene-h8, and the spectra are similar in appearance. The 0,0 transition was observed at  $29,020\text{ cm}^{-1}$  and the spectrum is depicted in Figure 4.3 .

g. Ortho-Deuterated Toluene

The spectrum of ortho-deuterated toluene, Figure 4.3 is not significantly different from that of toluene-h8 either. The 0,0 band was assigned as  $29,020\text{ cm}^{-1}$ , a value which is slightly to the blue of that for toluene-h8 and the wavenumber values of the 0,0 bands for the three monodeuterated toluenes are the same. The band assigned to the 0,a transition is shifted, appearing at  $1125\text{ cm}^{-1}$  while the same transition appeared at  $1165\text{ cm}^{-1}$  in toluene-h8. In the meta deuterated toluene, this transition is shifted only slightly, appearing at  $1155\text{ cm}^{-1}$ . The vibrational analysis of ortho-deuterated toluene is given in Table 4.5.

#### 4.2 DISCUSSION OF PHOSPHORESCENCE OF TOLUENE

The phosphorescence spectra of all the toluenes considered here are similar in appearance and the vibrational analysis of the parent is strongly reinforced by the analyses of the other molecules.

However, the phosphorescence spectra were quite different in appearance from the fluorescence (see Section 4.3). In the phosphorescence spectra, p forms only a very short progression while the longest progression is

in k. Schematic diagrams of both vibrational modes are presented in Figure (4.1) and it can be seen that they are somewhat complementary. For a molecule having an excited state geometry different from that of the ground state, the most prominent progression is in that mode which transforms the molecule from one geometry to the other.

The progressions in modes k and p, together with the lack of any progression in out of plane vibrations, imply that the excited triplet state is planar. The appearance of the progression in k is consistent either with a quinoidal geometry, i.e., the benzene ring having two short and four long bonds, with the methyl group at the apex of two of the long bonds, or with an antiquinoidal geometry. For toluene in a benzene matrix at 4°K, Haaland and Nieman<sup>10</sup> reported that the triplet state was quinoidally distorted, with a difference in length between long and short bonds of 0.035 Å. The lower resolution of the present spectra preclude a quantitative treatment as presented by these authors. Haaland and Nieman also estimated that the methyl group of toluene was out-of-the-plane of the ring by 3.6° in a benzene matrix at 4°K. The absence of out-of-plane vibrational progressions in methylcyclohexane matrix at 77°K suggests that the triplet state geometry of toluene is solvent-sensitive, as has been reported for benzene in various matrices. The main progression in toluene's phosphorescence is different from benzene's. There the main progression is in the breathing mode, indicating a hexagonal geometry with an overall increase in size.

Next, the prominence for the  $b_2$  false origin, mode l, in the phosphorescence spectrum of toluene will be discussed. It is necessary

first to recall the mechanism proposed for the phosphorescence of the parent, benzene. It has been suggested by Albrecht, that the  $T_1 \rightarrow S_0$ ,  ${}^3B_{1u} \rightarrow {}^1A_{1g}$  radiative transition in benzene arises from a second order mechanism,<sup>49</sup> wherein the lowest triplet state,  ${}^3B_{1u}$ , vibronically couples with a higher triplet state  ${}^3E_{1u}$ , which in turn spin-orbit couples with a  ${}^1A_{2u}$  singlet state, whose transition to the ground state is allowed. This pathway gives the lowest triplet state some  ${}^1A_{2u}$  character (the mixing of triplets into the ground singlet state is regarded as energetically unfeasible) and confers out-of-plane polarization on the phosphorescence. In other words, the phosphorescence is polarized like the singlet-singlet transition(s) that the triplet state "borrows" or "steals" intensity from. In-plane polarized phosphorescence is accounted for by replacing  ${}^1A_{2u}$  by  ${}^1E_{1u}$  in the above scheme. Experimentally, the phosphorescence of benzene is mainly out-of-plane polarized, suggesting the importance of the  ${}^1A_{2u}$  pathway. Direct first-order spin-orbit coupling in benzene is forbidden.

Turning to toluene, the first-order spin-orbit coupling term between the singlet states  $\Gamma_i$  and  $T_1$  (assumed to be  ${}^3A_1$ , as for other monosubstituted benzenes) is no longer forbidden. The transition moment due to this first order term is of the form

$$R_{T_1 \rightarrow S_0}^I = \sum_i R_{S_0 \rightarrow \Gamma_i} \times \frac{\langle {}^1\Gamma_i | H_{SO} | {}^3A_1 \rangle}{E({}^3A_1) - E({}^1\Gamma_i)} \times \langle \phi_k | \phi_0 \rangle \quad (4.1)$$

where  $R_{S_0 \rightarrow \Gamma_i}$  represents the transition moment of the  $S_i \rightarrow \Gamma_i$  process and  $\langle \phi_k | \phi_0 \rangle$  is the overlap integral between the  $k^{\text{th}}$  vibrational level of  $S_0$  and the zeroth vibrational level of the lowest triplet state.

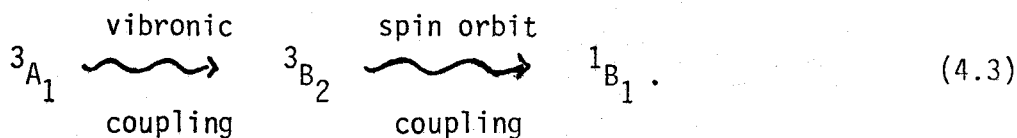
The latter integral vanishes unless the vibrational wavefunction  $\phi_k$  be-

longs to the totally symmetric representation. It should be noted that this type of term can only be responsible for transitions from  $T_1$  to totally symmetric vibrational levels of  $S_0$  or to vibrational levels of  $S_0$  where even multiples of non-totally symmetric vibrational are excited. The  ${}^1\Gamma_i$  states can be  ${}^1B_1$  and/or  ${}^1B_2$ .

The large intensity of one quantum of the non-totally symmetric  $b_2$  mode  $\ell$  in the phosphorescence spectrum has to be accounted for by a second order term in the spin-orbit coupling mechanism. If the second order mechanism for benzene mentioned above also holds for toluene, then one can write the transition moment due to this second order term as:

$$R_{T_1 \rightarrow S_0}^{II}(k) = \sum_{i,j} R_{S_i \rightarrow {}^1\Gamma_i} \times \frac{\langle {}^1\Gamma_i | H_{SO} | {}^3\Gamma_j \rangle}{E({}^3\Gamma_j) - E({}^1\Gamma_i)} \times \frac{\langle {}^3\Gamma_j | \frac{\partial H_0}{\partial Q,a} | {}^3A_1 \rangle}{E({}^3A_1) - E({}^3\Gamma_j)} \times \langle \phi_k | Q,a | \phi_0 \rangle \quad (4.2)$$

where  $Q,a$  represents the perturbing normal coordinate in the vibronic interaction, in this case mode  $\ell$ . The symmetry identification ( $b_2$ ) of mode  $\ell$  requires  $(\frac{\partial H_0}{\partial Q,a})$  to be of  $B_2$  symmetry and therefore  ${}^3\Gamma_j$  to be  ${}^3B_2$ . If  ${}^1\Gamma_i$  is  ${}^1B_1$ , which is the  ${}^1A_{2u}$  state of benzene lowered from  $D_{6h}$  to  $C_{2v}$  symmetry, then the intensity of mode  $\ell$  in the phosphorescence spectrum can be accounted for by a large contribution from  $R^{II}(\ell)$ :



The total transition probability  $P$  of the phosphorescence transition is:

$$P \propto \left[ \sum_k R^I(k)_{T_1 \rightarrow S_0} + \sum_k R^{II}(k)_{T_1 \rightarrow S_0} \right] \quad (4.4)$$

The summation occurs over all the vibrational bands of  $S_0$ , such as those presented in the vibrational analyses of the phosphorescence of toluene.

$R^{II}$  accounts for all the intensity in benzene and, in toluene, this term is also of prime importance, as can be seen by investigating the intensity of the  $R^I$  contributions versus that of the  $R^{II}$  contributions. Of course, it is impossible to give a quantitative evaluation to  $R^I/R^{II}$  from this work since bands do overlap and a given one can still have several contributions. The vibrational analysis lists the main contributions to the band. Nevertheless, qualitatively,  $R^{II}$  plays a much greater role than  $R^I$  in toluene. For example, the  $0,\ell$  band is about four times as intense as the  $0,0$  band. Methyl perturbation while giving a non-zero  $R^I$  contribution, still does not drastically change the fact that the vibronic spin-orbit pathway is still the dominant triplet intensity route. This result is in marked contrast to the phosphorescence of  $C_6H_5CCH$ ,<sup>50</sup>  $C_6H_5CN$ ,<sup>41</sup> and  $C_6H_5NC$ <sup>51</sup> studied in our laboratory, where the  $0,0$  transition is very intense, and the  $0,\ell$  transition was not observed. These latter three substituents seem to perturb benzene's triplet state much more than methyl does.

#### 4.3 VIBRATIONAL ANALYSIS OF FLUORESCENCE OF TOLUENES

It was found that  $10^{-3}$ - $10^{-4}$  M solutions of the toluenes in methylcyclohexane provided the sharpest spectra. At higher concentrations, the spectra were not well resolved and there was a decrease in intensities of the 0,0 bands due to self-absorption caused by the overlap of emission and absorption regions of the molecule. Spectra involving cyclohexane as solvent were quite resolved also but were not as detailed as those obtained with methylcyclohexane. The vibrational analyses presented here are for the toluenes in methylcyclohexane but the overall appearance of the spectra is not very different if cyclohexane is used as solvent.

##### a. Toluene-h8

The 0,0 band was of medium intensity and was assigned as  $37,320\text{ cm}^{-1}$ . The first intense band at  $775\text{ cm}^{-1}$  was assigned to the totally symmetric mode r and the most intense band in the spectrum was observed at  $985\text{ cm}^{-1}$ . It was assigned to the 0,p transition. The totally symmetric mode, q, was observed as a strong band at  $1220\text{ cm}^{-1}$ . At lower frequencies, two bands at  $520\text{ cm}^{-1}$  and  $625\text{ cm}^{-1}$  were attributed to a quantum of the totally symmetric mode, t, and a quantum of the  $b_2$  vibration s, respectively. The  $b_2$  mode u was observed at  $355\text{ cm}^{-1}$  but it was of very low intensity. The longest progression is in the ring breathing mode, p, up to  $0,5 \times p$  and there is another quite strong progression in r. Mode q enters into combinations with both progressions while the transition 0,s acts as a false origin for progressions in p and r. For example, four quanta of mode p are based on s.

The 0,0 band of the gas phase emission spectrum of toluene was

observed at  $37,474 \text{ cm}^{-1}$  by Kahane-Paillous and Leach.<sup>11</sup> With the exception of some low frequency vibrations, most fundamentals observed in that spectrum were also seen in this study. Watmann-Grajcar<sup>13</sup> assigned the 0,0 band of the toluene fluorescence spectrum with cyclohexane solvent as  $37,161.5 \text{ cm}^{-1}$  at  $77^\circ\text{K}$ . Bands at 123, 223, 286 and  $405 \text{ cm}^{-1}$  to the red of the origin were also observed in that spectrum but were not corroborated by this study. The  $123 \text{ cm}^{-1}$  band was attributed to a carbon-methyl torsional mode in their analyses. In the spectra of this study, where methylcyclohexane was used as solvent, a weak broad band was observed at  $355 \text{ cm}^{-1}$  and was assigned to the transition 0,u. In the spectra of toluene-h8 no splitting of spectral peaks due to solvent effects was observed. This state of affairs contrasts with the observations of workers who noticed splittings due to either the presence of the solvent in two crystalline modifications,<sup>29</sup> or to emission from solute molecules having different orientations within the solvent.<sup>26</sup> The spectrum is depicted in Figure 4.4 and the vibrational analysis is presented in Table 4.6 .

b. Toluene- $\alpha$ -d3

There is minimal difference between the fluorescence spectra of toluene- $\alpha$ -d3 and toluene-h8. The vibrational analysis of the former is also presented in Table 4.6 . In the spectrum of toluene- $\alpha$ -d3 the band assigned as 0,q ( $1225 \text{ cm}^{-1}$ ) is not as intense as in toluene-h8 and bands arising from combination of q with other progressions are weakened slightly. Secondly, the frequencies at  $1555 \text{ cm}^{-1}$  (assigned as 0,2xr) and  $1605 \text{ cm}^{-1}$  (0,p+s) of toluene-h8 are more widely separated

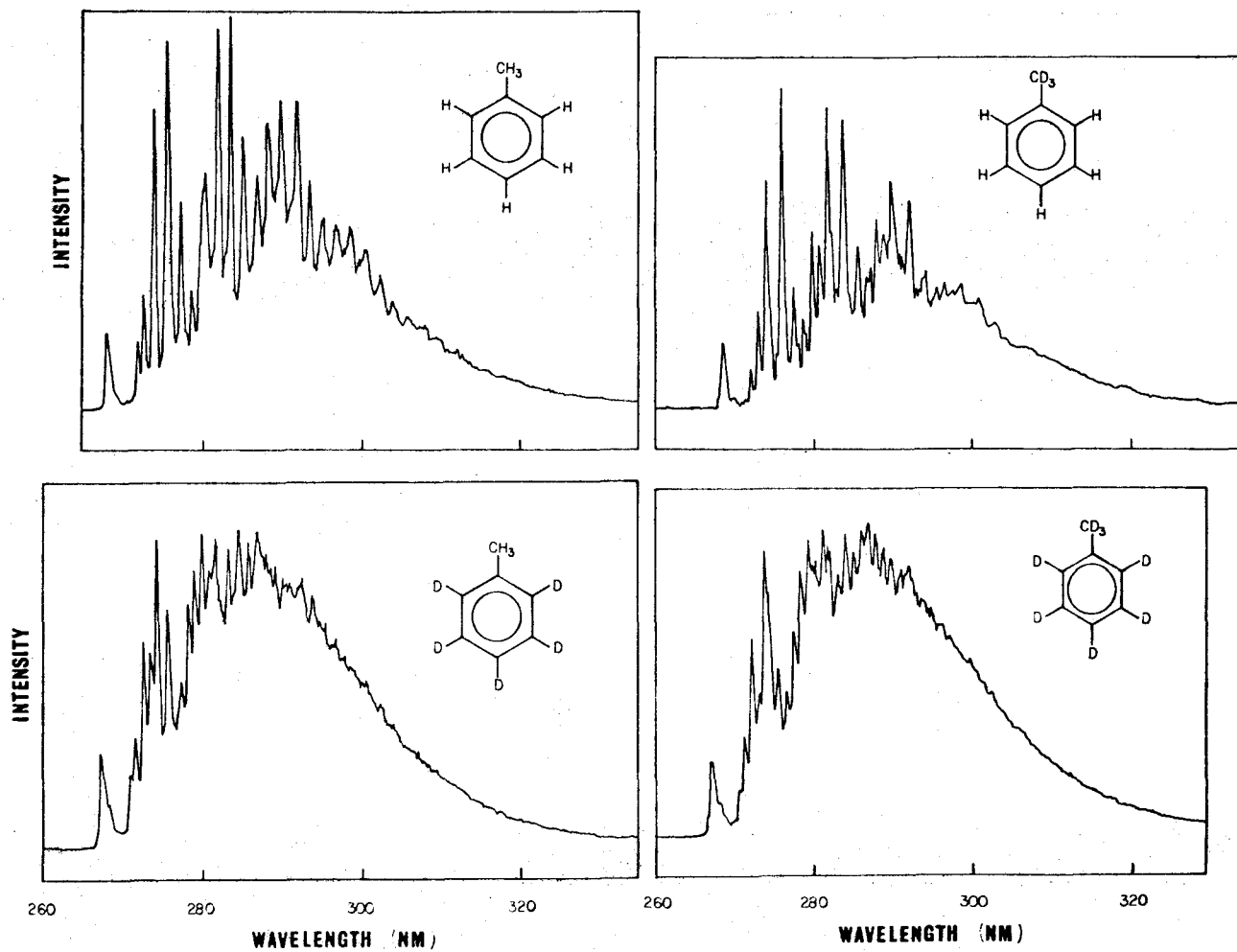


Figure 4.4 Fluorescence spectra of (clockwise from upper left) toluene-h8, toluene- $\alpha$ -d3, toluene-d8 and toluene-d5, all solutions  $10^{-3}$  M in methylcyclohexane matrices at 77°K.

TABLE 4.6

Vibrational Analyses of Fluorescences of  $10^{-3}$  M  $C_6H_5CH_3$  and  $10^{-3}$  M  $C_6H_5CD_3$   
in Polycrystalline Methylcyclohexane Matrices at 77°K.

| Toluene-h8          |                      | Toluene- $\alpha$ -d3 |             | Assignment <sup>a</sup> |
|---------------------|----------------------|-----------------------|-------------|-------------------------|
| $\nu$ ( $cm^{-1}$ ) | $\Delta\nu$          | $\nu$ ( $cm^{-1}$ )   | $\Delta\nu$ |                         |
| 37230               | 0                    | 37260                 | 0           | 0,0                     |
| 36875               | 355                  | 36930                 | 330         | 0,u                     |
| 36710               | 520                  | 36750                 | 510         | 0,t                     |
| 36605               | 625                  | 36645                 | 615         | 0,s                     |
| 36455               | 775                  | 36510                 | 750         | 0,r                     |
|                     |                      | 36445                 | 815         | 0,r'                    |
| 36245               | 1000                 | 36260                 | 1000        | 0,p                     |
| 36010               | 1205                 | 36035                 | 1225        | 0,q                     |
| 35930               | 1300 sh <sup>b</sup> | 35995                 | 1265 sh     | 0,r+t                   |
| 35830               | 1400                 | 35880                 | 1380        | 0,r+s                   |
| 35715               | 1515                 |                       |             | 0,p+t                   |
| 35675               | 1555                 | 35755                 | 1505        | 0,2xr                   |
| 35625               | 1605                 | 35640                 | 1620        | 0,p+s                   |
| 35575               | 1655 sh              | 35615                 | 1645 sh     | 0,s+2xt                 |
| 35450               | 1780                 | 35500                 | 1760        | 0,p+r                   |
|                     |                      | 35425                 | 1835 sh     | 0,p+r'                  |
| 35300               | 1930                 | 35335                 | 1925        | 0,r+s+t                 |
| 35235               | 1995                 | 35260                 | 2000        | 0,2xp;0,q+r             |
|                     |                      | 35235                 | 2025 sh     | 0,b+p                   |
| 35075               | 2155 sh              | 35150                 | 2110        | 0,2xr+s                 |
| 35040               | 2190                 | 35025                 | 2235        | 0,p+q                   |
| 34955               | 2275                 | 35000                 | 2260 sh     | 0,p+r+t                 |
| 34830               | 2400 sh              | 34870                 | 2390        | 0,p+r+s                 |
| 34805               | 2425                 | 34830                 | 2430        | 0,2xq                   |
| 34785               | 2445 sh              |                       |             | 0,r+s+2xt               |
| 34650               | 2580                 | 34745                 | 2515        | 0,2xr+p                 |

TABLE 4.6 (Continued)

| $\nu(\text{cm}^{-1})$ | $\Delta\nu$ | $\nu(\text{cm}^{-1})$ | $\Delta\nu$ | Assignment <sup>a</sup> |
|-----------------------|-------------|-----------------------|-------------|-------------------------|
| 34625                 | 2605        | 34640                 | 2620        | 0,2xp+s                 |
|                       |             | 34600                 | 2660        | 0,p+s+2xt               |
| 34520                 | 2710        | 34530                 | 2730 sh     | 0,p+q+t                 |
| 34470                 | 2760        | 34495                 | 2765        | 0,2xp+r;0,q+2xr         |
| 34445                 | 2785        | 34470                 | 2790        | 0,b+p+r                 |
| 34225                 | 3005        | 34260                 | 3000        | 0,3xp;0,p+q+r           |
| 34210                 | 3020        | 34235                 | 3025        | 0,b+2xp                 |
| 34035                 | 3195        | 34015                 | 3245        | 0,2xp+q                 |
| 33840                 | 3390        | 33820                 | 3440        | 0,p+2xq                 |
| 33625                 | 3605        | 33740                 | 3520        | 0,2xp+2xr               |
|                       |             | 33600                 | 3660        | 0,3xp+s                 |
| 33445                 | 3785        | 33500                 | 3760        | 0,3xp+r                 |
| 33235                 | 3995        | 33245                 | 4015        | 0,4xp;0,2xp+q+r         |
| 33035                 | 4195        | 33025                 | 4235        | 0,3xp+q                 |
| 32860                 | 4370        | 32840                 | 4420        | 0,2xp+2xq               |
| 32650                 | 4580        |                       |             | 0,4xp+s                 |
| 32445                 | 4785        | 32540                 | 4720        | 0,4xp+r                 |
| 32230                 | 5000        |                       |             | 0,5xp;0,3xp+q+r         |

<sup>a</sup> Designation of normal modes follows Whiffen.

<sup>b</sup> sh = shoulder

in toluene- $\alpha$ -d<sub>3</sub> because the former shifts to 1505  $\text{cm}^{-1}$  in this molecule. Of course, the 0,r transition is shifted from 775  $\text{cm}^{-1}$  in toluene-h<sub>8</sub> to 750  $\text{cm}^{-1}$  in toluene- $\alpha$ -d<sub>3</sub> so the assignment of 0,2xr is substantiated. A third difference is the appearance of a distinct shoulder at about 815  $\text{cm}^{-1}$  in toluene- $\alpha$ -d<sub>3</sub>. The transition causing it would have to undergo a dramatic shift in order to appear at 815  $\text{cm}^{-1}$  since, in toluene-h<sub>8</sub>, the peak assigned to 0,r is very sharp with no shoulders being evident. It is believed that the mode causing it is a ring-substituent rocking mode which can be either an out-of-plane mode, or a non-totally symmetric in-plane one. For toluene-h<sub>8</sub> the infrared frequency for this mode is  $\sim 1030 \text{ cm}^{-1}$  (refer to Table 4.1) and since vibration p(1000  $\text{cm}^{-1}$ ) is very intense in the fluorescence spectrum, the rocking mode frequency is probably buried under it. When the spectra of the two molecules are run at comparable signal to noise ratios, the toluene- $\alpha$ -d<sub>3</sub> spectrum shows a peak at 1000  $\text{cm}^{-1}$  which is much sharper than that of the toluene-h<sub>8</sub> spectrum. It is therefore believed that the ring substituent bending mode shifts to 815  $\text{cm}^{-1}$  upon deuteration of the methyl group. In spite of these differences, the overall appearances of the fluorescence spectra is similar for both molecules. The 0,0 transition for the toluene- $\alpha$ -d<sub>3</sub> spectrum was assigned as 37,260  $\text{cm}^{-1}$  and the spectrum is depicted in Figure 4.4 .

#### c. Toluene-d<sub>8</sub>

The fluorescence spectrum of toluene-d<sub>8</sub> is shown in Figure and the vibrational analysis is listed in Table 4.7 . The 0,0 transition was observed at 37,410  $\text{cm}^{-1}$  which is to be compared with the

TABLE 4.7

Vibrational Analyses of Fluorescences of  $10^{-3}$  M  $C_6D_5CH_3$  and  $10^{-3}$  M  $C_6D_5CD_3$   
in Polycrystalline Methylcyclohexane Matrices at 77°K.

| Toluene-d5            |                      | Toluene-d8            |             | Assignment <sup>a</sup>    |
|-----------------------|----------------------|-----------------------|-------------|----------------------------|
| $\nu(\text{cm}^{-1})$ | $\Delta\nu$          | $\nu(\text{cm}^{-1})$ | $\Delta\nu$ |                            |
| 37385                 | 0                    | 37410                 | 0           | 0,0                        |
| 37245                 | 140                  | 37245                 | 165         | 0,lattice                  |
| 36875                 | 510                  | 36915                 | 495         | 0,t                        |
| 36790                 | 595                  | 36820                 | 590         | 0,s                        |
| 36655                 | 730                  | 36700                 | 710         | 0,r                        |
|                       |                      | 36670                 | 740 sh      |                            |
| 36535                 | 850                  | 36565                 | 845         | 0,b or 0,r' in toluene-d-8 |
| 36430                 | 955                  | 36455                 | 955         | 0,p                        |
|                       |                      | 36415                 | 995 sh      | 0,2xt                      |
| 36245                 | 1140                 | 36245                 | 1165        | 0,q                        |
| 36050                 | 1335                 | 36100                 | 1310        | 0,r+s                      |
| 36025                 | 1360                 |                       |             | 0,b+t                      |
| 35930                 | 1455                 | 35995                 | 1415        | 0,2xr                      |
| 35830                 | 1555                 | 35870                 | 1540        | 0,p+s                      |
| 35805                 | 1580 sh <sup>b</sup> |                       |             | 0,b+r                      |
| 35700                 | 1685                 | 35755                 | 1655        | 0,p+r                      |
| 35675                 | 1710 sh              | 35665                 | 1745        | 0,q+s                      |
| 35575                 | 1810                 | 35625                 | 1785        | 0,b+p                      |
| 35485                 | 1900                 | 35525                 | 1885        | 0,2xp                      |
| 35425                 | 1960 sh              | 35425                 | 1985        | 0,b+q                      |
| 35300                 | 2085                 | 35275                 | 2135        | 0,p+q                      |
| 35110                 | 2275                 | 35150                 | 2260        | 0,p+r+s                    |
| 35090                 | 2295                 |                       |             | 0,2xq                      |
| 34975                 | 2410                 | 35025                 | 2385        | 0,p+2xr                    |
| 34855                 | 2530                 | 34905                 | 2505        | 0,2xp+s                    |
| 34830                 | 2555                 |                       |             | 0,b+p+r                    |

TABLE 4.7 (Continued)

| $\nu(\text{cm}^{-1})$ | $\Delta\nu$ | $\nu(\text{cm}^{-1})$ | $\Delta\nu$ | Assignment <sup>a</sup> |
|-----------------------|-------------|-----------------------|-------------|-------------------------|
| 34785                 | 2600        | 34805                 | 2605        | 0,2xp+r                 |
| 34700                 | 2685        |                       |             | 0,p+q+s                 |
| 34640                 | 2745        | 34685                 | 2725        | 0,b+2xp                 |
| 34555                 | 2830        | 34565                 | 2845        | 0,3xp                   |
| 34425                 | 2960        | 34445                 | 2965        | 0,b+p+q                 |
| 34340                 | 3045        | 34330                 | 3080        | 0,2xp+q                 |
| 34175                 | 3210        | 34210                 | 3200        | 0,2xp+r+s               |
|                       |             | 34095                 | 3315        | 0,2xp+2xr               |
| 33990                 | 3395        | 33965                 | 3445        | 0,3xp+s                 |
| 33840                 | 3545        | 33840                 | 3570        | 0,3xp+r                 |
|                       |             | 33695                 | 3715        | 0,b+3xp                 |
| 33590                 | 3795        | 33615                 | 3795        | 0,4xp                   |
| 33435                 | 3950        |                       |             | 0,3xp+q                 |
| 33265                 | 4120        | 33255                 | 4155        | 0,3xp+r+s               |
| 33035                 | 4350        |                       |             | 0,4xp+s                 |
| 32875                 | 4510        | 32895                 | 4515        | 0,4xp+s                 |
|                       |             | 32660                 | 4750        | 0,5xp                   |

<sup>a</sup> Designation of normal modes follows Whiffen.

<sup>b</sup> sh = shoulder

37,351.0  $\text{cm}^{-1}$  value assigned by Watmann-Grajcar, who used cyclohexane solvent at 77°K.<sup>13</sup> Fundamental frequencies at 102, 198, 297, 337 and 400  $\text{cm}^{-1}$  were also observed in that work but no definite bands appeared below 500  $\text{cm}^{-1}$  in the toluene-d8 fluorescence spectrum of this study. The band at 845  $\text{cm}^{-1}$  could be assigned to the methyl group rocking mode r', but mode b is probably a larger contributor. As is the case in toluene-h8, the main progressions are in the  $a_1$  modes p and r but the bands are broadened and somewhat less intense than their counterparts in toluene-h8. The 0,p transition moves from 1000  $\text{cm}^{-1}$  in toluene-h8 to 955  $\text{cm}^{-1}$  in this molecule while 0,r shifts from 775  $\text{cm}^{-1}$  to 710  $\text{cm}^{-1}$  in toluene-d8. Perdeuteration also caused the bands at 625 and 520  $\text{cm}^{-1}$  to shift to 590 and 495  $\text{cm}^{-1}$ , respectively. These isotope shifts are consistent with those expected on the basis of infrared and Raman data for toluene-h8 and toluene-d8 (refer to Table 4.1) and serve to substantiate the assignments presented here for toluene-h8 fluorescence.

#### d. Toluene-d5

The fluorescence spectrum of toluene-d5 is similar to that of toluene-d8. It should be noted, however, that the toluene-d5 spectrum is sharper and that the band assigned to mode q is not only sharper but much more intense than it was in toluene-d8. The band assigned to 0,p is very sharp and there are no shoulders associated with it. The principal features of the spectrum are the intense progressions in r and p, with the  $b_2$  mode s acting as a false origin. The vibrational analysis is given in Table 4.7 and the spectrum is depicted in Figure 4.4. The 0,0 band appears at 37,385  $\text{cm}^{-1}$ .

e. Para-deuterated toluene

Deuteration at the para position causes the 0,0 value to change only slightly from  $37,230\text{ cm}^{-1}$  to  $37,245\text{ cm}^{-1}$ . The overall appearance of the spectrum is similar to that of toluene-h8 because the progressions in p and r remain the most prominent feature of the spectrum. There are shoulders at 790, 830, 1015 and  $1235\text{ cm}^{-1}$  which could be caused by the glass emissions if the sample is not totally polycrystalline. However, it is more likely that they are due to emission from toluene-h8 impurity because the wavelength values of the shoulders correspond, within experimental error, to those of toluene-h8.

The h8 transition 0,b could be contributing intensity to the shoulder at  $1015\text{ cm}^{-1}$  since, according to infrared data (Refer to Table (4.1)), it has a wavenumber value in this region. Other prominent bands in the spectrum had shoulders which were attributed to toluene-h8. The vibrational analysis is presented in Table 4.8 and the spectrum is shown in Figure 4.5.

f. Meta-deuterated toluene

The wavenumber value of the 0,0 transition of meta-deuterated toluene is  $37,260\text{ cm}^{-1}$  which is  $30\text{ cm}^{-1}$  to the blue of that for toluene-h8. The spectrum resembles that of para-deuterated toluene with only minor differences. The shoulders which appeared at 790 and  $830\text{ cm}^{-1}$  in para-deuterated toluene, are resolved as individual peaks in the spectrum of the meta compound where they appeared at 790 and  $855\text{ cm}^{-1}$  respectively. The 0,r transition appears at  $750\text{ cm}^{-1}$  and 0,2xr is also shifted so that it overlaps with 0,p+t at  $1520\text{ cm}^{-1}$ . Many of the shoulders which were assigned to toluene-h8 in the para fluorescence

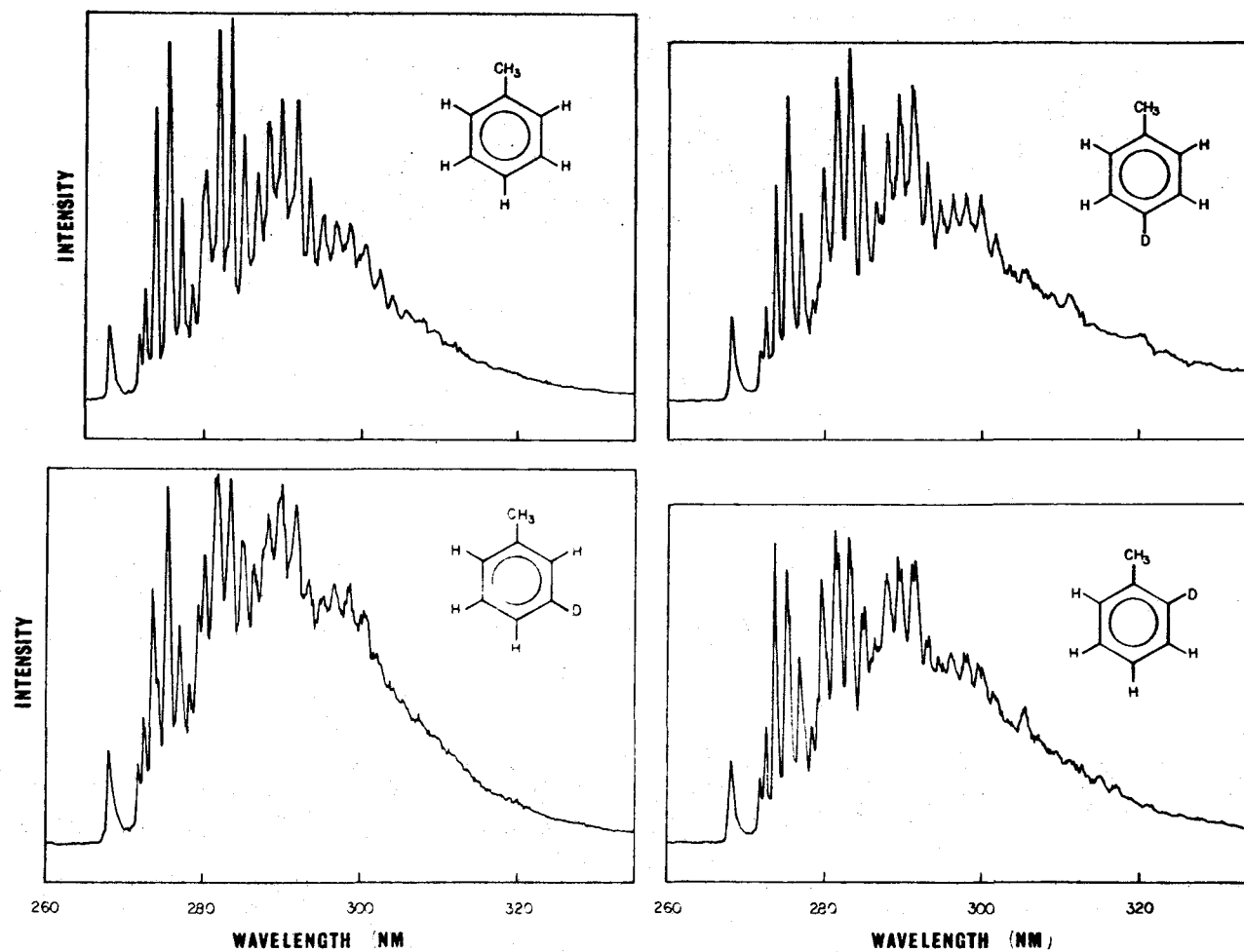


Figure 4.5 Fluorescence spectra of (clockwise from upper left) toluene-h<sub>8</sub>, para, ortho and meta-deuterated toluenes, all solutions 10<sup>-3</sup> M in methylcyclohexane matrices at 77°K.

TABLE 4.8  
 Vibrational Analyses of Fluorescences of  $10^{-3}$  M para-D-C<sub>6</sub>H<sub>5</sub>CH<sub>3</sub>,  $10^{-3}$  M meta-D-C<sub>6</sub>H<sub>5</sub>CH<sub>3</sub> and  
 $10^{-3}$  M ortho-D-C<sub>6</sub>H<sub>5</sub>CH<sub>3</sub> in Polycrystalline Methylcyclohexane Matrices at 77°K .

| para-d-Toluene        |                     | meta-d-Toluene        |             | ortho-d-Toluene       |             | Assignment <sup>a</sup> |
|-----------------------|---------------------|-----------------------|-------------|-----------------------|-------------|-------------------------|
| $\nu(\text{cm}^{-1})$ | $\Delta\nu$         | $\nu(\text{cm}^{-1})$ | $\Delta\nu$ | $\nu(\text{cm}^{-1})$ | $\Delta\nu$ |                         |
| 37245                 | 0                   | 37260                 | 0           | 37260                 | 0           | 0,0                     |
| 36915                 | 315                 | 36915                 | 345         | 36930                 | 330         | 0,u                     |
| 36740                 | 505                 | 36740                 | 520         | 36750                 | 510         | 0,t                     |
| 36645                 | 600                 | 36655                 | 605         | 36645                 | 615         | 0,s                     |
| 36485                 | 760                 | 36510                 | 750         | 36485                 | 775         | 0,r                     |
| 36455                 | 790 sh <sup>b</sup> | 36470                 | 790         | 36445                 | 815 sh      | h8 imp. <sup>c</sup>    |
| 36415                 | 830 sh              | 36405                 | 855         | 36405                 | 855 sh      |                         |
| 36260                 | 985                 | 36260                 | 1000        | 36260                 | 1000        | 0,p                     |
| 36230                 | 1015                | 36230                 | 1030        | 36230                 | 1030        | h8 imp.;0,b             |
| 36035                 | 1210                | 36060                 | 1200        | 36060                 | 1200        | 0,q                     |
| 36010                 | 1235 sh             | 36035                 | 1225 sh     | 36025                 | 1235 sh     | h8 imp.                 |
| 35985                 | 1260 sh             | 35995                 | 1265 sh     | 35985                 | 1275 sh     | 0,r+t                   |
| 35870                 | 1375                | 35895                 | 1365        | 35870                 | 1390        | 0,r+s                   |
| 35755                 | 1490                | 35740                 | 1520        | 35755                 | 1505 sh     | 0,p+t                   |
| 35665                 | 1580 sh             |                       |             | 35690                 | 1570        | 0,2xr                   |
| 35650                 | 1595                | 35640                 | 1620        | 35640                 | 1620        | 0,p+s                   |
| 35585                 | 1660 sh             | 35615                 | 1645 sh     | 35615                 | 1645 sh     | h8 imp.                 |
| 35475                 | 1770                | 35500                 | 1760        | 35485                 | 1775        | 0,p+r                   |
| 35450                 | 1795 sh             | 35460                 | 1800        | 35450                 | 1810        | h8 imp.;0,b+r           |
|                       |                     | 35410                 | 1850 sh     | 35400                 | 1860 sh     |                         |

TABLE 4.8 (Continued)

| $\nu(\text{cm}^{-1})$ | $\Delta\nu$ | $\nu(\text{cm}^{-1})$ | $\Delta\nu$ | $\nu(\text{cm}^{-1})$ | $\Delta\nu$ | Assignment <sup>a</sup> |
|-----------------------|-------------|-----------------------|-------------|-----------------------|-------------|-------------------------|
|                       |             | 35300                 | 1960 sh     |                       |             |                         |
| 35285                 | 1960        | 35275                 | 2005        | 35275                 | 1985        | 0,2xp;0,q+r             |
| 35260                 | 1985 sh     | 35235                 | 2025        | 35250                 | 2010        | h8 imp.;0,b+p           |
| 35050                 | 2195        | 35050                 | 2210        | 35075                 | 2185        | 0,p+q                   |
| 35025                 | 2220 sh     | 35015                 | 2245        | 35015                 | 2245        | h8 imp.                 |
| 34975                 | 2270 sh     |                       |             |                       |             |                         |
| 34870                 | 2375        | 34880                 | 2380        | 34880                 | 2380        | 0,p+r+s                 |
| 34845                 | 2400        | 34845                 | 2415 sh     | 34870                 | 2390        | 0,2xq                   |
|                       |             | 34770                 | 2490 sh     | 34805                 | 2455        | h8 imp.                 |
| 34710                 | 2535        | 34745                 | 2515        | 34700                 | 2560        | 0,p+2xr                 |
| 34685                 | 2560        | 34660                 | 2600        | 34640                 | 2620 sh     | 0,2xp+s                 |
| 34625                 | 2620 sh     | 34625                 | 2635 sh     |                       |             | h8 imp.                 |
| 34540                 | 2705 sh     | 34540                 | 2720 sh     | 34555                 | 2705 sh     | 0,p+q+t                 |
| 34505                 | 2740        | 34505                 | 2755        | 34505                 | 2755        | 0,2xp+r;0,q+2xr         |
| 34470                 | 2775        | 34445                 | 2815        | 34460                 | 2800        | 0,b+p+r;0,p+q+s         |
|                       |             | 34410                 | 2850        | 34410                 | 2850 sh     | h8 imp.;0,b+q+s         |
| 34315                 | 2930 sh     | 34315                 | 2945        | 34315                 | 2945 sh     |                         |
| 34280                 | 2965 sh     | 34245                 | 3015        | 34270                 | 2990        | 0,3xp;0,p+q+r           |
| 34235                 | 3010 sh     | 34210                 | 3050 sh     | 34235                 | 3025        | h8 imp.;0,b+2xp         |
|                       |             |                       |             | 34200                 | 3060 sh     | h8 imp.                 |
| 34085                 | 3160        | 34070                 | 3190        | 34085                 | 3175        | 0,2xp+q                 |
| 34050                 | 3195 sh     | 34025                 | 3235        | 34050                 | 3210        | h8 imp.;0,b+p+q         |
| 33850                 | 3395        | 33850                 | 3410        | 33875                 | 3385        | 0,p+2xq                 |
| 33820                 | 3425 sh     |                       |             | 33840                 | 3420        | h8 imp.                 |

TABLE 4.8 (Continued)

| $\nu(\text{cm}^{-1})$ | $\Delta\nu$ | $\nu(\text{cm}^{-1})$ | $\Delta\nu$ | $\nu(\text{cm}^{-1})$ | $\Delta\nu$ | Assignment <sup>a</sup> |
|-----------------------|-------------|-----------------------|-------------|-----------------------|-------------|-------------------------|
|                       |             |                       |             | 33705                 | 3555        | 0,2xp+2xr               |
| 33695                 | 3550        | 33680                 | 3580        | 33635                 | 3625 sh     | 0,3xp+s                 |
| 33510                 | 3735        | 33510                 | 3750        | 33510                 | 3750        | 0,3xp+r                 |
| 33480                 | 3765 sh     | 33465                 | 3795        | 33465                 | 3795        | h8 imp.                 |
| 33290                 | 3955        | 33245                 | 4015        | 33780                 | 3980        | 0,4xp                   |
| 33235                 | 4010 sh     |                       |             |                       |             | h8 imp.                 |
|                       |             | 33090                 | 4170        |                       |             |                         |
| 33080                 | 4165        | 33035                 | 4225        | 33080                 | 4180        | 0,3xp+q                 |
| 33035                 | 4210 sh     |                       |             |                       |             | h8 imp.                 |
| 32875                 | 4370        | 32860                 | 4400        | 32875                 | 4385        | 0,2xp+2xq;0,3xp+r+s     |
| 32660                 | 4585        | 32690                 | 4570        | 32680                 | 4580        | 0,4xp+s                 |
| 32530                 | 4715        | 32500                 | 4760        | 32500                 | 4760        | 0,4xp+r                 |
| 32330                 | 4915        | 32250                 | 5010        | 32280                 | 4970        | 0,5xp;0,3xp+q+r         |

<sup>a</sup> Designation of normal modes follows Whiffen.

<sup>b</sup> sh = shoulder

<sup>c</sup> Toluene-h8 impurity.

spectrum were also seen in the spectrum of the meta compound. The vibrational analysis, which is much like that of para-deuterated toluene is presented in Table 4.8 and the spectrum is presented in Figure 4.5 .

g. Ortho-deuterated toluene

Placing deuterium in the ortho position causes the 0,0 transition to shift  $40 \text{ cm}^{-1}$  to the blue of that for toluene-h8 so that it is at  $37,260 \text{ cm}^{-1}$ . The band at  $775 \text{ cm}^{-1}$ , assigned as 0,r, is slightly more intense than that due to 0,p whereas in all other molecules of this study mode p was the most intense of the fluorescence fundamentals. The vibrational analysis of this molecule is also given in Table 4.8 and the fluorescence spectrum is illustrated in Figure 4.5 .

#### 4.4 DISCUSSION OF FLUORESCENCE OF TOLUENE

According to the vibrational analyses of the fluorescence spectra, the most prominent progression involves the ring breathing mode, p. There is also a moderately long progression in r, and q combines with both progressions. The schematic representations of r and p in Figure 4.1 show that these two modes are complementary to each other. The length of the progression in these two modes implies that, in the first excited singlet state, toluene has a slightly expanded regular hexagon structure. The lack of progression in out-of-plane vibrations implies that the molecule is planar in the first excited singlet state. This behaviour is similar to that reported for benzene whose C-C bond length increases by  $0.037 \text{ \AA}$  when the molecule enters the first excited singlet state.

In Section 2.8, it was stated that in cases where an electronic transition was forbidden, the symmetry selection rule (equation (2.14))

was not valid. The more general vibronic selection rule

$$R_{e'v'e''v''} = \langle \psi_{e'v'} | M | \psi_{e''v''} \rangle \quad (2.12)$$

$R_{e'v'e''v''}$  being the vibronic transition moment, applies in such instances.

If the vibronic transition moment is to be non-zero, the direct product of the irreducible representations of the two vibronic states must contain the irreducible representation of at least one of the components of  $M$ . In order to obtain the irreducible representation of the vibronic state, one takes the direct product of the irreducible representations of the electronic state and of the vibrational normal mode involved.

In benzene (point group  $D_{6h}$ ), the first excited singlet, or  $S_1$  state, is of  $B_{2u}$  symmetry while  $S_0$  transforms as  $E_{1u}$ . The direct product of the former with  $e_{2g}$  yields the latter representation so that, if an  $e_{2g}$  vibration is excited, the two electronic states mix and transitions between the totally symmetric ground state and  $S_1$ , which is now a vibronic state, can occur. This can be written as,

$$R_{e'v'e''v''} = \langle A_{1g} a_{1g} | M | B_{2u} e_{2g} \rangle \neq 0 \quad (4.5)$$

and

$$A_{1g} \otimes a_{1g} \otimes B_{2u} \otimes e_{2g} = \Gamma_{M_x, M_y} \quad (4.6)$$

In this manner, absorption from the zeroth vibrational level of  $S_0$  ( ${}^1A_{1g}$ ) to vibronic states of  $S_1$  that have a symmetry of  $B_{2u} \otimes e_{2g} = E_{1u}$  is accounted for.

The fluorescence of benzene, from the zeroth vibrational level of  $S_1$  ( ${}^1B_{2u}$ ) to vibronic levels of  $S_0$  is also allowed according to the following integral:

$$R_{e'v'e''v''} = \langle A_{1g} e_{2g} | M | B_{2u} a_{1g} \rangle \neq 0. \quad (4.7)$$

For benzene the  $e_{2g}$  ground state vibration required occurs at  $606 \text{ cm}^{-1}$  and the fluorescence spectrum includes this vibronic component. The pure electronic component is rigorously forbidden, but may in fact occur very weakly if the molecule is in a crystal or lattice where field effects could cause slight relaxation of symmetry restrictions.

The methyl group in toluene does not represent a strong perturbation on the ring but the overall symmetry of the molecule has decreased (point group  $C_{2v}$ ); the pure electronic component of the spectrum is allowed and equation (2.14) can be written:

$$R_{e'e''} = \langle \psi' | M | \psi'' \rangle \neq 0 \quad (2.14)$$

where  $\Gamma_{\psi'} \otimes \Gamma_{\psi''} = A_1, B_1$  or  $B_2$ . The  $S_0 \leftrightarrow S_1$ ,  ${}^1A_1 \leftrightarrow {}^1B_2$  transition is allowed via  $M_y$  which transforms as  $B_2$ . Nevertheless, the vibronic character inherited from the parent benzene is still evident as the intensity of the 0,0 transition is equal to that of the false origin at  $620 \text{ cm}^{-1}$ . This band is due to normal mode  $s$  which transforms as  $b_2$ . Then,

$$A_1 \otimes a_1 \otimes B_2 \otimes b_2 = \Gamma_{M_z}. \quad (4.8)$$

In other words, the vibronic false origin band is z-polarized while the 0,0 band is y-polarized. The  $b_2$  band does not appear in the toluene fluorescence spectrum, a situation which contrasts with that observed in the phosphorescence spectrum of that molecule.

It is true that the "allowedness" of transitions is governed

by rules formulated from group theory. However, the intensity of a forbidden component is determined, in part, by the size of the energy gap between the excited electronic states which are mixing. For example, in ethynylbenzene the mixing of excited states  $S_1$  and  $S_2$  is strong because the  $S_1$ - $S_2$  energy gap is only 0.65 e.v. The corresponding energy gap in phenylisocyanide is 0.83 e.v. so  $S_1$  and  $S_2$  are perturbing each other strongly in this molecule also. However, in benzonitrile and toluene, the difference in energy between  $S_1$  and  $S_2$  is approximately 1 e.v. so the vibronic components of the spectra of these two molecules are reduced in intensity compared with the corresponding component in the fluorescence spectrum of ethynylbenzene and phenylisocyanide.

#### 4.5 VIBRATIONAL ANALYSIS OF FLUORESCENCE OF BENZYL RADICALS

##### a. Benzyl-h7

The 0,0 transition of h7 is of medium intensity and in this study was observed at  $21,655 \text{ cm}^{-1}$ . Watmann-Grajcar<sup>13</sup> analyzed the fluorescence spectrum of h7 using cyclohexane as solvent at  $77^\circ\text{K}$  and found that the 0,0 band appeared at  $21,666.9 \text{ cm}^{-1}$ . The fluorescence spectra of benzyl- $\alpha$ -d2 and benzyl-d7 were obtained under the same conditions and analyzed but the vibronic structure was complicated in all three molecules by the presence of peak splittings due to solute molecules emitting from the monoclinic and cubic environments which coexist in the sample. Furthermore, Watmann-Grajcar observed nine low frequency vibrations between the 0,0 (monoclinic) and  $531 \text{ cm}^{-1}$ . One of those bands was assigned as the 0,0 transition from solute molecules trapped in a cubic lattice while several more transitions were attributed to lattice vibrations. The weak band at  $230 \text{ cm}^{-1}$  was ascribed to benzyl radicals trapped in an environment containing predominantly toluene molecules. Three fundamentals were assigned at  $361 \text{ cm}^{-1}$ ,  $393 \text{ cm}^{-1}$  and  $435 \text{ cm}^{-1}$  with the band at  $361 \text{ cm}^{-1}$  being the most intense of the three. Furthermore, there were bands which were described as "satellite bands", that is bands arising from the coupling of lattice vibrations with vibrational modes of the solute. Ripoche,<sup>22</sup> however, observed the 0,0 at  $21,647 \text{ cm}^{-1}$  for the benzyl-h7 fluorescence and recorded only one low frequency band at  $362 \text{ cm}^{-1}$  when methylcyclohexane was used as solvent at liquid air temperature. In addition, Lloyd and Wood<sup>52</sup> recently reported the  $21,682 \text{ cm}^{-1}$  band as the fluorescence 0,0 for benzyl-h7 in an adamantane matrix. The only low frequency vibrational mode noticed

in their work was assigned at  $365\text{ cm}^{-1}$ . A similar result was obtained in this study where the band at  $355\text{ cm}^{-1}$  was assigned as 0,u. The two most intense bands of the spectrum, at  $525\text{ cm}^{-1}$  and  $620\text{ cm}^{-1}$  were assigned as 0,t and 0,s respectively while the 0,l transition also gives rise to a prominent band in the spectrum. Bands due to modes r, p and q also appear but they are of low intensity. Modes r, p, t and l form short progressions with no more than two quanta of any of these vibrations appearing.

The allowed component of the spectrum includes the moderately intense 0,0 band, the 0,t transition (very intense) and 0,p (weak). The forbidden, or vibronic component is based upon the very intense 0,s transition at  $620\text{ cm}^{-1}$  which transforms as  $b_2$ . Finally the  $b_2$  model  $\ell$  enters into combinations with modes t, s, r and p. The fluorescence spectrum of benzyl-h7 is shown in Figure 4.6 and the vibrational analysis is presented in Table 4.9. The results of that analysis tend to confirm the work of Ripoche<sup>22</sup> and Lloyd et al.<sup>52</sup>

b. Benzyl- $\alpha$ -d2

There is little difference between the vibrational analysis of benzyl- $\alpha$ -d2 and that of benzyl-h7. The use of methylcyclohexane as solvent enabled relatively uncomplicated spectra to be acquired because, in contrast with cyclohexane systems, there were fewer peak splittings and "satellite" bands present. Watmann-Grajcar<sup>13</sup> observed the 0,0 transition at  $21,645.8\text{ cm}^{-1}$  and assigned three low frequency modes at  $321\text{ cm}^{-1}$ ,  $354\text{ cm}^{-1}$ , and  $411\text{ cm}^{-1}$  respectively where cyclohexane was used as the solvent at  $77^\circ\text{K}$ . In the spectra studied here, the 0,0 band was assigned as  $21,630\text{ cm}^{-1}$  and it was

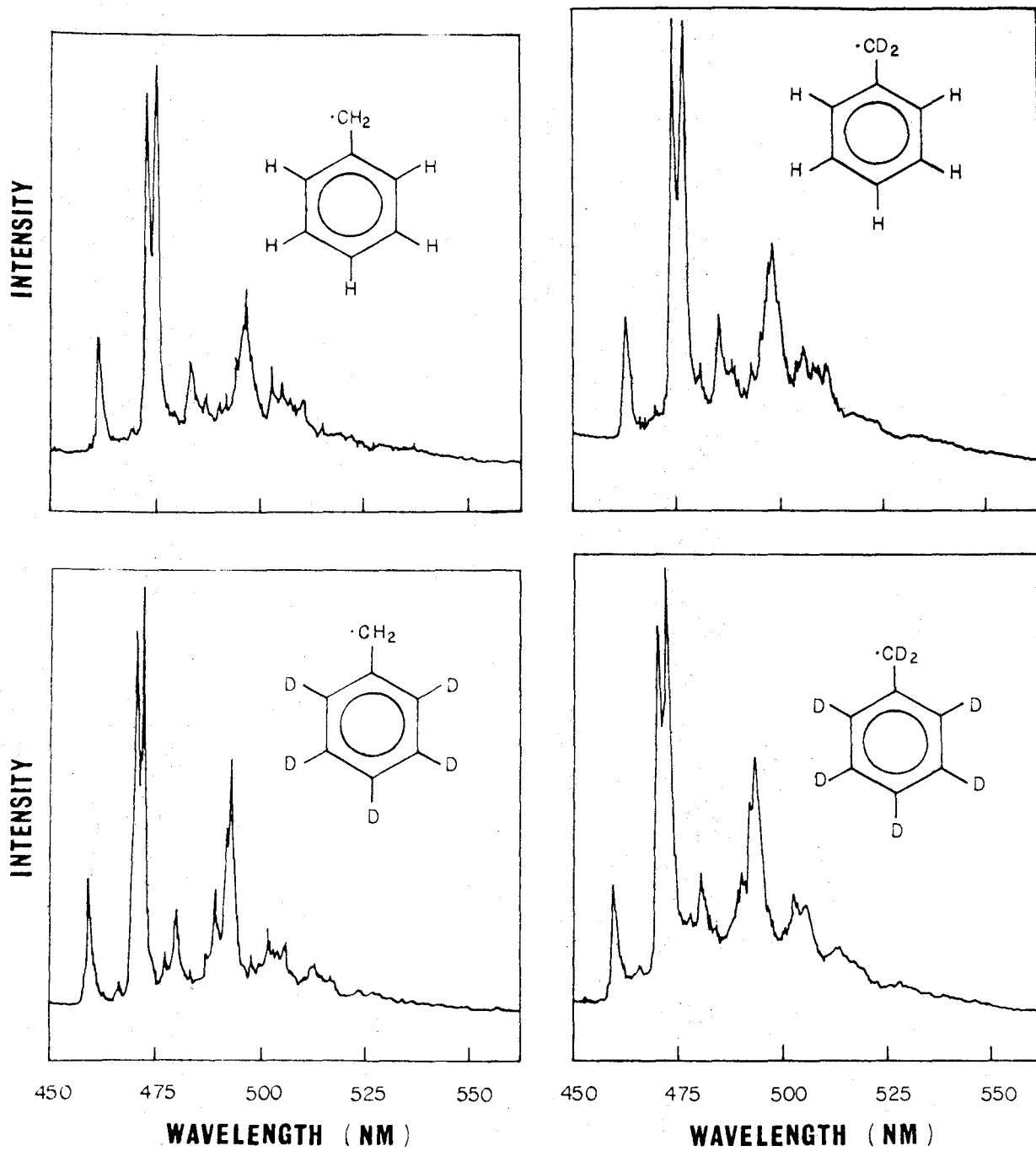


Figure 4.6 Fluorescence spectra of (clockwise from upper left) benzyl -h<sub>7</sub>, benzyl- $\alpha$ -d<sub>2</sub>, benzyl-d<sub>7</sub> and benzyl-d<sub>5</sub> radicals in methylcyclohexane matrices at 77°K.

TABLE 4.9

Vibrational Analysis of Fluorescences of  $C_6H_5CH_2\cdot$ , and  $C_6H_5CD_2\cdot$   
in Polycrystalline Methylcyclohexane Matrices at 77°K.

| Benzyl Radical-h7   |                     | Benzyl Radical- $\alpha$ -d2 |             | Assignment <sup>a</sup> |
|---------------------|---------------------|------------------------------|-------------|-------------------------|
| $\nu$ ( $cm^{-1}$ ) | $\Delta\nu$         | $\nu$ ( $cm^{-1}$ )          | $\Delta\nu$ |                         |
| 21655               | 0                   | 21630                        | 0           | 0,0                     |
| 21610               | 50                  | 21585                        | 45          | lattice                 |
| 21485               | 170                 |                              |             | lattice                 |
| 21405               | 250                 | 21390                        | 240         |                         |
| 21300               | 355                 | 21310                        | 320         | 0,u                     |
| 21130               | 525                 | 21125                        | 505         | 0,t                     |
| 21035               | 620                 | 21025                        | 605         | 0,s                     |
| 20845               | 810                 | 20850                        | 780         | 0,r                     |
| 20805               | 850                 |                              |             | 0,t+u                   |
| 20665               | 990                 | 20650                        | 980         | 0,p                     |
| 20625               | 1030                | 20600                        | 1030        | 0,b;0,2xt               |
| 20515               | 1140                | 20505                        | 1125        | 0,s+t                   |
| 20385               | 1270                | 20360                        | 1270        | 0,q                     |
| 20315               | 1340                | 20315                        | 1315        | 0,r+t                   |
| 20220               | 1435                | 20220                        | 1410        | 0,r+s                   |
| 20145               | 1510                | 20140                        | 1490        | 0,p+t                   |
| 20115               | 1540                | 20090                        | 1540        | 0, $\ell$               |
| 20035               | 1620sh <sup>b</sup> | 20045                        | 1585        | 0,p+s                   |
| 19865               | 1790                | 19860                        | 1770        | 0,p+r;0,q+t             |
| 19780               | 1875                | 19805                        | 1825        | 0,q+s                   |
| 19690               | 1965                | 19675                        | 1955        | 0,2xp                   |
| 19595               | 2060                | 19580                        | 2050        | 0, $\ell$ +t            |
| 19510               | 2145                | 19525                        | 2105        | 0,p+s+t;0, $\ell$ +s    |
| 19420               | 2235                |                              |             | 0,p+q                   |
| 19300               | 2355                | 19325                        | 2305        | 0, $\ell$ +r            |
| 19140               | 2515                | 19130                        | 2500        | 0, $\ell$ +p            |
| 18875               | 2780                | 18865                        | 2765        | 0,2xp+r                 |

<sup>a</sup> Designation of normal modes follows Whiffen.

<sup>b</sup> sh = shoulder

noted that modes u, t, s and r shifted slightly to  $320\text{ cm}^{-1}$ ,  $505\text{ cm}^{-1}$ ,  $605\text{ cm}^{-1}$  and  $780\text{ cm}^{-1}$  respectively. In spite of such shifts, the overall appearance of the fluorescence spectrum is similar to that of benzyl-h7. The vibrational analysis of the benzyl- $\alpha$ -d2 fluorescence spectrum is also contained in Table 4.9 and the spectrum is presented in Figure 4.6.

c. Benzyl-d7

The fluorescence spectrum of this molecule is presented in Figure 4.6 and Table 4.10 contains the vibrational analysis. The 0,0 transition shifts  $120\text{ cm}^{-1}$  to the blue upon perdeuteration of benzyl-h7, so that this band appears at  $21,735\text{ cm}^{-1}$ . This value compares favorably with those determined by Ripoché<sup>22</sup> and Watmann-Grajcar<sup>13</sup> who observed the 0,0 bands of their systems at  $21,737\text{ cm}^{-1}$  and  $21,756.6\text{ cm}^{-1}$  respectively. Watmann-Grajcar noticed several low frequency modes below  $400\text{ cm}^{-1}$  but Ripoché observed only the 0,u transition at  $300\text{ cm}^{-1}$ . The appearance of 0,u at that frequency is affirmed by this study but no other low frequency modes were observed in the benzyl-d7 spectra considered here. The overall appearance of the spectrum is not very different from that of benzyl-h7 although all fundamentals present are shifted considerably. The 0,b transition, which appears at  $1030\text{ cm}^{-1}$  in benzyl-h7, shifts to  $835\text{ cm}^{-1}$  in the benzyl-d7 spectrum while modes t, s, r and p shift from  $525\text{ cm}^{-1}$ ,  $620\text{ cm}^{-1}$ ,  $810\text{ cm}^{-1}$  and  $990\text{ cm}^{-1}$  to  $495\text{ cm}^{-1}$ ,  $580\text{ cm}^{-1}$ ,  $770\text{ cm}^{-1}$  and  $940\text{ cm}^{-1}$  respectively. The 0,l transition shifts from  $1540\text{ cm}^{-1}$  in benzyl-h7 to  $1480\text{ cm}^{-1}$  in benzyl-d7. The magnitudes of these shifts are similar to those observed for the corresponding modes of toluene when it is perdeuterated. As in benzyl-h7, the 0,t and 0,s transitions are the

TABLE 4.10

Vibrational Analysis of Fluorescences of  $C_6D_5CH_2\cdot$  and  $C_6D_5CD_2\cdot$   
in Polycrystalline Methylcyclohexane Matrices at 77°K.

| Benzyl Radical-d5     |                                 | Benzyl Radical-d7     |             | Assignment <sup>a</sup> |
|-----------------------|---------------------------------|-----------------------|-------------|-------------------------|
| $\nu(\text{cm}^{-1})$ | $\Delta\nu$                     | $\nu(\text{cm}^{-1})$ | $\Delta\nu$ |                         |
| 21765                 | 0                               | 21735                 | 0           | 0,0                     |
| 21580                 | 185                             | 21565                 | 170         | lattice                 |
|                       |                                 | 21490                 | 245         |                         |
| 21425                 | 340                             | 21435                 | 300         | 0,u                     |
| 21255                 | 510                             | 21240                 | 495         | 0,t                     |
| 21180                 | 585                             | 21155                 | 580         | 0,s                     |
| 20995                 | 770                             | 20965                 | 770         | 0,r                     |
| 20925                 | 840                             | 20900                 | 835         | 0,b                     |
| 20815                 | 950                             | 20795                 | 940         | 0,p                     |
| 20665                 | 1100                            | 20660                 | 1075        | 0,s+t                   |
| 20505                 | 1260                            | 20480                 | 1255        | 0,r+t                   |
| 20455                 | 1310                            | 20415                 | 1320        | 0,b+t                   |
| 20415                 | 1350                            | 20375                 | 1360        | 0,r+s                   |
| 20310                 | 1455                            | 20295                 | 1445        | 0,p+t                   |
| 20270                 | 1495                            | 20255                 | 1480        | 0,l                     |
|                       |                                 | 20235                 | 1500        |                         |
| 20245                 | 1520 <sup>sh</sup> <sup>b</sup> | 20220                 | 1515        | 0,p+s                   |
| 20145                 | 1620                            | 20125                 | 1610        | 0,b+r                   |
| 20045                 | 1720                            |                       |             | 0,p+r                   |
| 19970                 | 1795                            |                       |             | 0,b+p                   |
| 19895                 | 1870                            | 19865                 | 1870        | 0,2xp                   |
| 19865                 | 1900                            | 19840                 | 1895        |                         |
| 19820                 | 1945                            | 19840                 | 1895        | 0,b+s+t                 |
|                       |                                 | 19785                 | 1950        |                         |
| 19745                 | 2020                            | 19745                 | 1990        | 0,l+t                   |
| 19725                 | 2040                            | 19700                 | 2035        | 0,p+s+t                 |
| 19660                 | 2105                            | 19645                 | 2090        | 0,b+r+t                 |
| 19480                 | 2285                            | 19455                 | 2280        | 0,l+r                   |
| 19325                 | 2440                            | 19315                 | 2420        | 0,l+p                   |
| 18920                 | 2845                            |                       |             | 0,3xp                   |

<sup>a</sup> Designation of normal modes follows Whiffen.

<sup>b</sup> sh = shoulder

most intense in the spectrum and the transition due to the ring breathing mode  $p$  is weak. There are progressions in modes  $r$ ,  $p$  and  $l$  but they are very short.

d. Benzyl-d5

The fluorescence spectrum of benzyl-d5 is almost identical to that of benzyl-d7 (see Figure 4.6). The vibrational analysis is presented in Table 4.10 and it is quite similar to the one provided for benzyl-d7. The 0,0 band was observed at  $21765 \text{ cm}^{-1}$  and fundamental modes  $u$ ,  $t$ ,  $s$ ,  $r$ ,  $b$  and  $p$  appear. The most intense bands are due to the 0,t and 0,s transitions while 0,p is quite weak.

e. Para-Deuterated Benzyl Radical

Placing a deuterium atom in the para position in benzyl radical causes negligible change in the frequency of the 0,0 band which appears at  $21660 \text{ cm}^{-1}$ . The overall appearance of the spectrum is similar to that of the benzyl-h7 fluorescence although the peaks are broadened slightly in the region between  $1300 \text{ cm}^{-1}$  and  $1600 \text{ cm}^{-1}$ . There are several shoulders in the spectrum which are believed to be due to benzyl-h7 impurity emission. The most intense bands in the spectrum are again due to the totally symmetrical mode  $t$  and the non-totally symmetric, in-plane mode  $s$ . The frequency values of the fundamental modes are shifted only slightly in para-deuterated benzyl radicals so the vibrational analysis presented for benzyl-h7 is still essentially valid. The analysis is given in Table 4.11 and the fluorescence spectrum is depicted in Figure 4.7.

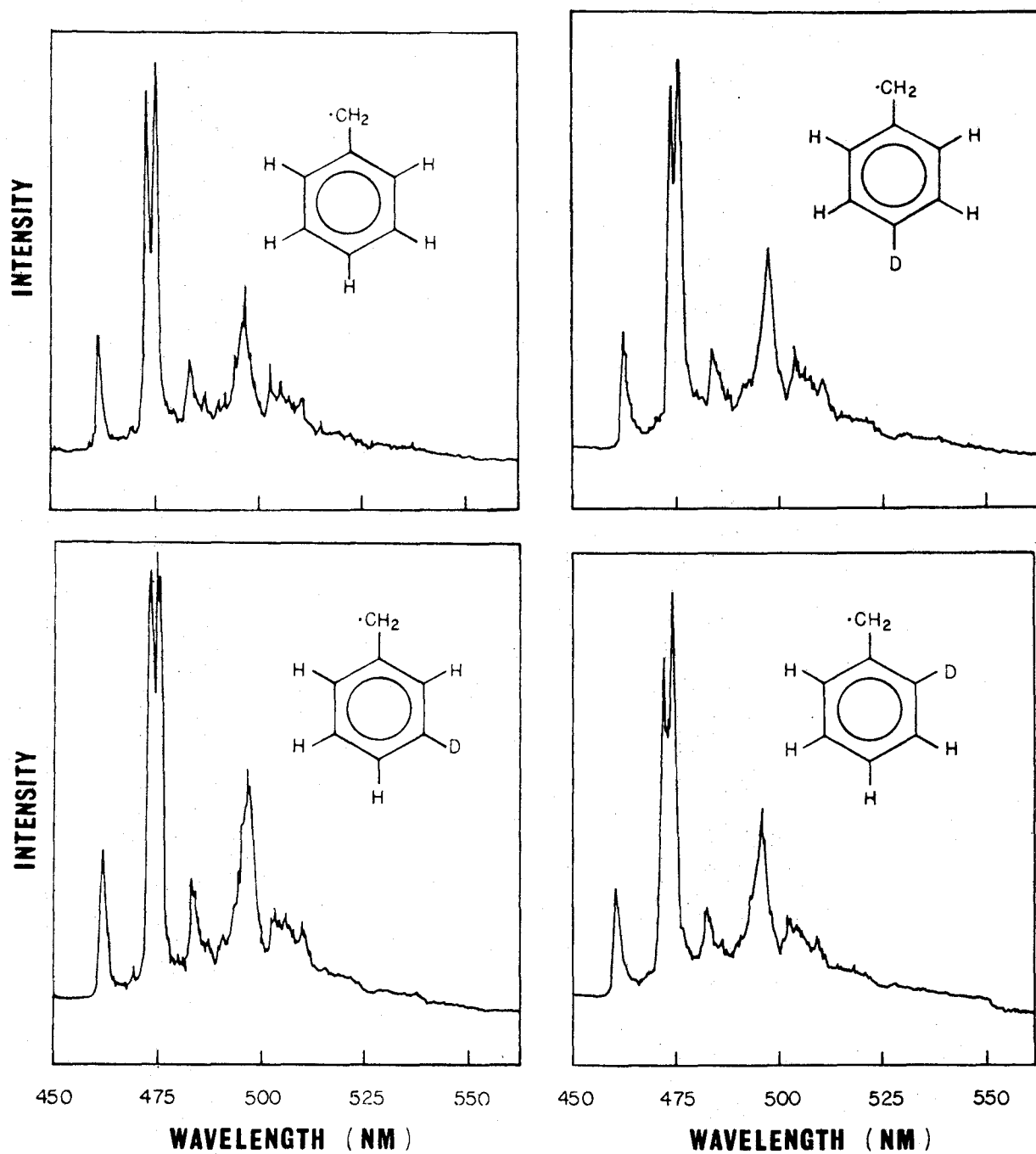


Figure 4.7 Fluorescence spectra of (clockwise from upper left)benzyl-h7, para, ortho and meta-deuterated benzyl radicals in methylcyclohexane matrices at 77°K.

Table 4.11

Vibrational Analysis of Fluorescences of p-D-C<sub>6</sub>H<sub>4</sub>CH<sub>2</sub>·, m-D-C<sub>6</sub>H<sub>4</sub>CH<sub>2</sub>· and o-D-C<sub>6</sub>H<sub>4</sub>CH<sub>2</sub>·  
in Polycrystalline Methylcyclohexane Matrices at 77°K.

| para-d-Benzyl Radical |                   | meta-d-Benzyl Radical |             | ortho-d-Benzyl Radical |             | Assignment <sup>a</sup> |
|-----------------------|-------------------|-----------------------|-------------|------------------------|-------------|-------------------------|
| $\nu(\text{cm}^{-1})$ | $\Delta\nu$       | $\nu(\text{cm}^{-1})$ | $\Delta\nu$ | $\nu(\text{cm}^{-1})$  | $\Delta\nu$ |                         |
| 21660                 | 0                 | 21670                 | 0           | 21685                  | 0           | 0,0                     |
|                       |                   | 21655                 | 15          | 21665                  | 20          | h7 imp <sup>c</sup>     |
| 21605                 | 55sh <sup>b</sup> | 21610                 | 60          | 21620                  | 65          | lattice                 |
| 21515                 | 145               | 21515                 | 155         | 21515                  | 170         | lattice                 |
| 21300                 | 360               | 21305                 | 365         | 21325                  | 360         | 0,u                     |
| 21135                 | 525               | 21140                 | 530         | 21165                  | 520         | 0,t                     |
|                       |                   | 21130                 | 540         | 21135                  | 550sh       | h7 imp.                 |
| 21045                 | 615               | 21660                 | 610         | 21070                  | 615         | 0,s                     |
|                       |                   | 21045                 | 625         |                        |             | h7 imp.                 |
| 20860                 | 800               | 20885                 | 795         | 20885                  | 800         | 0,r                     |
| 20685                 | 975               | 20685                 | 985         | 20700                  | 985         | 0,p                     |
| 20625                 | 1035sh            | 20625                 | 1045sh      | 20645                  | 1040sh      | 0,b;0,2xt               |
| 20535                 | 1125              | 20530                 | 1140        | 20545                  | 1140        | 0,s+t                   |
| 20405                 | 1255              | 20395                 | 1275        | 20410                  | 1275        | 0,q                     |
| 20340                 | 1320              | 20365                 | 1305        | 20345                  | 1340        | 0,r+t                   |
| 20220                 | 1440              | 20270                 | 1400        | 20265                  | 1420        | 0,r+s                   |
|                       |                   | 20220                 | 1450sh      | 20220                  | 1465sh      | h7 imp.                 |
| 20160                 | 1500sh            | 20165                 | 1505sh      | 20175                  | 1510sh      | 0,p+t                   |

Table 4.11 (cont'd)

| para-d-Benzyl Radical |             | meta-d-Benzyl Radical |             | ortho-d-Benzyl Radical |             | Assignment   |
|-----------------------|-------------|-----------------------|-------------|------------------------|-------------|--------------|
| $\nu(\text{cm}^{-1})$ | $\Delta\nu$ | $\nu(\text{cm}^{-1})$ | $\Delta\nu$ | $\nu(\text{cm}^{-1})$  | $\Delta\nu$ |              |
| 20135                 | 1525        | 20140                 | 1530sh      | 20145                  | 1540        | 0, $\ell$    |
| 20115                 | 1545sh      | 20115                 | 1555sh      | 20115                  | 1570sh      | H7 imp.      |
| 20085                 | 1575sh      | 20085                 | 1585sh      | 20085                  | 1600        | 0,p+s        |
| 20030                 | 1630sh      | 20055                 | 1615        |                        |             | H7 imp.      |
| 19875                 | 1785        | 19900                 | 1775        | 19895                  | 1790        | 0,p+r;0,q+t  |
|                       |             | 19865                 | 1805        | 19860                  | 1815        | H7 imp.      |
| 19805                 | 1855        | 19780                 | 1875        | 19800                  | 1885        | 0,q+s        |
| 19720                 | 1940        | 19720                 | 1950        | 19710                  | 1975        | 0,2xp        |
| 19615                 | 2045        | 19620                 | 2050        | 19620                  | 2065sh      | 0, $\ell$ +t |
| 19590                 | 2070sh      | 19585                 | 2085sh      | 19585                  | 2100sh      | H7 imp.      |
| 19530                 | 2130        | 19535                 | 2135        | 19540                  | 2145        | 0,p+s+t      |
| 19435                 | 2225        | 19400                 | 2270        | 19435                  | 2250        | 0,p+q        |
|                       |             |                       |             | 19325                  | 2360        | 0, $\ell$ +r |
| 19170                 | 2490        | 19155                 | 2515        | 19180                  | 2505        | 0, $\ell$ +p |
| 18910                 | 2750        | 18915                 | 2755        | 18925                  | 2760        | 0,2xp+r      |

<sup>a</sup> Designation of normal modes follows Whiffen.

<sup>b</sup> sh - shoulder

<sup>c</sup> Benzyl-h7 impurity

f. Meta-Deuterated Benzyl Radical

The vibrational analysis of the fluorescence of this molecule is also contained in Table 4.11 and the spectrum is shown in Figure 4.7 . The 0,0 transition is slightly blue shifted to  $21,670 \text{ cm}^{-1}$ . In the spectrum of this molecule, peaks due to benzyl-h7 impurity emission are more noticeable than was the case with the para-deuterated benzyl radical spectrum. The appearance of the spectrum is similar to that of the fluorescence of the para compound since bands due to the 0,t and 0,s transition remain the most intense ones. The vibrational analysis is very much like that for the para deuterated benzyl radical fluorescence.

g. Ortho-Deuterated Benzyl Radical

The 0,0 band is blue shifted by  $30 \text{ cm}^{-1}$  so it appears at  $21,685 \text{ cm}^{-1}$  in the fluorescence of this molecule. However, the other fundamentals present in the spectrum are shifted only slightly, if at all, from their frequency values in the benzyl-h7 spectrum. In the spectra of the benzyl radical molecules considered here, the bands assigned to transition 0,t ( $520 \text{ cm}^{-1}$ ) and 0,s ( $615 \text{ cm}^{-1}$ ) are of comparable intensity. In ortho-deuterated benzyl radical however, the 0,t band is somewhat less intense than that assigned to 0,s. Table 4.11 contains the vibrational analysis while the fluorescence spectrum is the subject of Figure 4.7.

#### 4.6 DISCUSSION OF FLUORESCENCE OF BENZYL RADICAL

Bindley and Walker<sup>17</sup> investigated the emission spectrum observed between  $4400\text{\AA}$  and  $5000\text{\AA}$  after treatment of toluene by an electric discharge. They were able to show that the spectrum was due to benzyl radical emission. They observed isotope shifts in some bands of the radical emission spectrum

when toluene- $\alpha$ -d<sub>3</sub> was used in the discharge instead of toluene itself. The radical substituents were found to be -CH<sub>2</sub> when toluene-h<sub>8</sub> was used in the discharge and -CD<sub>2</sub> if toluene- $\alpha$ -d<sub>3</sub> was employed.

The ground state of benzyl radical is a doublet and has B<sub>1</sub> symmetry. For a time there was some argument as to whether the first excited state had A<sub>2</sub> or B<sub>1</sub> symmetry. The photoselection experiments of Johnson and Albrecht<sup>53</sup> indicated that the symmetry of this state was B<sub>1</sub> but Cossart-Magos and Leach<sup>19</sup> performed rotational contour analyses on several bands of the gas phase emission spectra of benzyl-h<sub>7</sub>, benzyl- $\alpha$ -d<sub>2</sub> and benzyl-d<sub>7</sub>, concluding that the first excited state of benzyl was of A<sub>2</sub> symmetry. Friedrich and Albrecht,<sup>24</sup> after further photoselection measurements, reached the same conclusion.

Longuet-Higgins and Pople<sup>54</sup> predicted qualitatively that there should be two absorption systems in the visible and near UV regions of the spectrum and that the higher energy one, involving a  ${}^2B_1$ - ${}^2B_1$  transition should have the greater intensity. Baudet<sup>55</sup> calculated the oscillator strength of the  ${}^2B_1$ - ${}^2B_1$  transition as  $1.8 \times 10^{-2}$  while that of the  ${}^2A_2$ - ${}^2B_1$  transition was found to be  $3.2 \times 10^{-3}$ . An approximate calculation of the oscillator strength of the  ${}^2A_2$ - ${}^2B_1$  transition was carried out by Laposa and Morrison<sup>56</sup> who used fluorescence lifetime data as the basis of the calculation and a value of  $\sim 8 \times 10^{-4}$  was determined by them. These oscillator strength values indicate that, while the pure electronic transition  ${}^2A_2$ - ${}^2B_1$

is allowed on group theoretical grounds, it will be of very low intensity. In addition, a portion of the intensity of the transition can be accounted for in terms of a vibronic factor:

$$R_{e'v'e''v''} = \langle A_2 a_1 | M | B_1 b_2 \rangle \neq 0 \quad (4.9)$$

and

$$A_2 \otimes a_1 \otimes B_1 \otimes b_2 = A_1 \equiv \Gamma_{M_z} \quad (4.10)$$

This can account for the presence of mode  $s$ , acting as a false origin.

The main features of the benzyl radical fluorescence spectrum, then, are the weakly allowed 0,0 transition, the very strong 0,t ( $525 \text{ cm}^{-1}$ ) transition which is allowed in the same sense as the 0,0 one and the 0,s ( $620 \text{ cm}^{-1}$ ) transition, which serves as a false origin. The fundamental frequencies of benzyl radical are not very different from those of other monosubstituted benzenes, particularly toluene. They can therefore be assigned quite reliably,<sup>17</sup> although the benzyl radical itself cannot be produced in the large concentrations required to obtain the vibrational fundamental frequencies from infrared and Raman experiments. According to the selection rules given previously, the vibronic contribution to the spectrum can be due to  $b_1$ ,  $b_2$  or  $a_1$  vibrational modes if the first excited electronic state is of  $B_1$  symmetry. If that state is an  $A_2$  state, then the vibrations contributing to the vibronic term can be of  $a_1$ ,  $a_2$  or  $b_2$  symmetry. All bands in the benzyl radical spectra of this study were assigned to  $a_1$  or  $b_2$  vibrational modes while neither  $b_1$  nor  $a_2$  modes appeared. It is known that at  $77^\circ\text{K}$  most transitions involved in emission spectra originate at the lowest vibrational level of the first excited

electronic state (see section 2.10). Unfortunately, the vibrational analysis of benzyl radical fluorescence presented here cannot distinguish between  $A_2$  or  $B_1$  symmetry for the first excited state although work previously mentioned has established it as  $A_2$ . The results presented here are consistent with that result although the  $a_2$  vibrations cited by Watmann-Grajcar<sup>13</sup> as a basis for assigning that symmetry according to vibronic selection rules did not appear in the spectra studied here. Ripoche<sup>22</sup> observed an  $a_2$  vibration at  $865\text{ cm}^{-1}$  for benzyl-h7 in cyclopentane, methylcyclopentane and methylcyclohexane solvent but was unable to affirm it in the corresponding benzyl-d7 spectra. The bands assigned to  $a_2$  transitions with cyclohexane solvent could be due to other fundamentals coupling with lattice modes.

It is interesting to compare the benzyl radical fluorescence spectrum with that of toluene. In both molecules, the pure electronic transition is only weakly allowed. In toluene, however, the  $520\text{ cm}^{-1}$  and  $625\text{ cm}^{-1}$  bands are roughly equal in intensity to that of the 0,0 transition whereas in the benzyl radical spectrum, the bands at  $520$  and  $625\text{ cm}^{-1}$  are much more intense than the 0,0 transition. The second excited state is much closer in energy to the first one in benzyl radical than it is in toluene so that the first order vibronic term could become relatively large and this fact is reflected in the intensity of the vibronic part of the spectrum. In toluene, totally symmetric modes p and r give rise to strong bands and there is a long progression of up to five quanta involving the o,p transition. In the benzyl radical fluorescence, the o,r transition is very weak and o,p does not originate long progressions although it is

of noticeable intensity. As was mentioned in the discussion of toluene fluorescence (section 4.4), the long progression in the ring breathing mode,  $\nu_1$ , enables one to argue, on the basis of the Franck-Condon principle that in the first excited singlet state, the molecule is planar but expanded slightly. A similar conclusion cannot be achieved regarding the geometry of benzyl radical in the first excited doublet state as the progressions in the fluorescence spectrum involved are very short. The conclusions arrived at on the basis of the spectra analyzed in this study are similar to those obtained by Watmann-Grajcar<sup>13</sup> and Ripoche.<sup>22</sup>

## CHAPTER V

### SUMMARY

The phosphorescence and fluorescence spectra of toluene and some of its deuterated analogues in polycrystalline methylcyclohexane matrices at 77°K were recorded. The phosphorescence spectra and their corresponding vibrational analyses are similar for all these toluenes but differ from the fluorescence spectra and vibrational analyses obtained under the same conditions.

The vibrational analyses of the fluorescence spectra are consistent with a planar, slightly expanded hexagon structure for the toluenes in the first excited singlet state.

The phosphorescence spectra indicate that the triplet state geometry of toluene is planar in polycrystalline methylcyclohexane matrix. As in the case of benzene, the lowest triplet state geometry of toluene is solvent sensitive.

The fluorescence spectra of benzyl radical and its deuterated analogues in polycrystalline methylcyclohexane matrices were also recorded. The progressions in these spectra were quite short and the vibrational analyses were obtained by using fundamental modes and frequencies analogous to those observed in toluene fluorescence under the same conditions.

Forbidden components were prominent in the spectra of all three systems. In the toluene phosphorescence, and also in the benzyl radical

fluorescence, the vibronic origin was found to be much more intense than the pure electronic one. In the toluene fluorescence spectra, on the other hand, the vibronic and electronic origins were of comparable intensity.

## REFERENCES

1. D.P. Craig, J. Chem. Soc., 1950, 2146.
2. J.B. Coon, R.E. DeWames and C.M. Loyd, J. Mol. Spectrosc., 8, 285 (1962).
3. G.C. Nieman, J. Chem. Phys., 50, 1674 (1969).
4. H. Sponer, J. Chem. Phys., 10, 672 (1942).
5. N. Ginsburg, W.W. Robertson and F.A. Matsen, J. Chem. Phys., 14, 511 (1946).
6. R.K. Asundi and M.R. Padhye, Ind. J. Phys., 23, 331 (1949).
7. D.F. Evans, J. Chem. Soc., 1959, 2753.
8. Y. Kanda and R. Shimada, Spectrochim. Acta, 17, 279 (1961).
9. Y. Kanda and H. Sponer, J. Chem. Phys., 28, 798 (1958).
10. D.M. Haaland and G.C. Nieman, J. Chem. Phys. 59, 4435 (1973).
11. J. Kahane-Paillous and S. Leach, J. Chim. Phys., 55, 439 (1958).
12. A.M. Bass, J. Chem. Phys., 18, 1403 (1950).
13. L. Vatmann-Grajcar, J. Chim. Phys., 66, 1023 (1969).
14. H. Schuler, L. Reinebeck and R. Koberle, Z. Naturforschg., 7a, 421 (1952).
15. H. Schuler and A. Michel, Z. Naturforschg., 10a, 439 (1955).
16. H. Schuler and J. Kusjakow, Spectrochim. Acta, 17, 356 (1961).
17. J.F. Bindley and S. Walker, Trans. Faraday Soc., 58, 217 (1962).
18. A.T. Watts and S. Walker, J. Chem. Soc., 1962, 4323.
19. C. Cossart-Magos and S. Leach, J. Chem. Phys., 56, 1534 (1972).
20. I. Norman and G. Porter, Proc. Roy. Soc. (London), A230, 399 (1955).

21. G. Porter and E. Strachan, *Spectrochim. Acta*, 12, 299 (1958).
22. J. Ripoché, *Spectrochim. Acta*, 23A, 1003 (1967).
23. D.M. Friedrich and A.C. Albrecht, *Chem. Phys.*, 6, 366 (1974).
24. D.M. Friedrich and A.C. Albrecht, *J. Chem. Phys.*, 58, 4766 (1973).
25. F.A. Keidel and S.H. Bauer, *J. Chem. Phys.*, 25, 1218 (1956).
26. H.D. Rudolph, H. Driezler, A. Jaeschke and P. Wendling, *Z. Naturforschg.*, 22a, 940 (1967).
27. R.S. Mulliken, *J. Chem. Phys.*, 23, 1997 (1955).
28. E.B. Wilson, J.C. Decius and P.C. Cross, *Molecular Vibrations*, McGraw-Hill, New York, 1955.
29. G. Herzberg, *Electronic Spectra of Polyatomic Molecules*, Van Nostrand, Princeton, New Jersey, 1966.
30. G.W. King, *Spectroscopy and Molecular Structure*, Holt, Rinehart and Winston, New York, 1964.
31. G. Herzberg, *Electronic Spectra of Diatomic Molecules*, Van Nostrand, Princeton, New Jersey, 1950.
32. M. Born and R. Oppenheimer, *Ann. d. Physik.*, 84, 457 (1927).
33. G. Herzberg and E. Teller, *Z. Physik. Chem.*, B21, 410 (1933).
34. M. Kasha, *Discussions Faraday Soc.*, 9, 14 (1950).
35. M. Kasha, *Radiation Res.*, Suppl. 2, 243 (1960).
36. G.W. Robinson, *J. Mol. Spectrosc.*, 6, 58 (1961).
37. G.W. Robinson and R.P. Frosch, *J. Chem. Phys.*, 37, 1962 (1962).
38. G.W. Robinson and R.P. Frosch, *J. Chem. Phys.*, 38, 1187 (1963).
39. B. Meyer, *Low Temperature Spectroscopy*, American Elsevier Publishing Co., New York, 1971.

40. J.D. Spangler and N.G. Kilmer, *J. Chem. Phys.*, 48, 698 (1968).
41. G.L. Lebel and J.D. Laposa, *J. Mol. Spectrosc.*, 41, 249 (1972).
42. N.H. Werstiuk and T. Kadai, *Can. J. Chem.*, 51, 1485 (1973).
43. G.L. Lebel, J.D. Laposa, B.G. Sayer, and R.A. Bell, *Anal. Chem.*, 43, 1500 (1971).
44. D.H. Whiffen, *J. Chem. Soc.*, 1956, 1350.
45. E.B. Wilson, *Phys. Rev.*, 45, 706 (1934).
46. G. Varsanyi, *Assignments for Vibrational Spectra of Seven Hundred Benzene Derivatives*, Adam Hilger, 1974.
47. A. Hitchcock and J.D. Laposa, *J. Mol. Spectrosc.*, 54, 223 (1975).
48. N. Fuson, C. Garrigou-Lagrange and M.L. Josien, *Spectrochim. Acta*, 16, 106 (1960).
49. A.C. Albrecht, *J. Chem. Phys.*, 38, 354 (1963).
50. H. Singh and J.D. Laposa, *J. Luminescence*, 3, 287 (1971).
51. R. Nalepa and J.D. Laposa, *J. Luminescence*, 8, 429 (1974).
52. R.V. Lloyd and D.E. Wood, *J. Chem. Phys.*, 60, 2684 (1974).
53. P.M. Johnson and A.C. Albrecht, *J. Chem. Phys.*, 48, 851 (1968).
54. H.C. Longuet-Higgins and J.A. Pople, *Proc. Phys. Soc.*, 68A, 591 (1955).
55. J. Baudet and M. Suard, *J. Chim. Phys.*, 67, 1088 (1970).
56. J.D. Laposa and V. Morrison, *Chem. Phys. Lett.*, 28, 270 (1974).